An Experimental Study of an Offshore Platform

Brincker, Rune; Asmussen, John Christian; Andersen, Palle ; Kirkegaard, Poul Henning

Publication date:
1994

Document Version
Early version, also known as pre-print

INSTITUTTET FOR BYGNINGSTEKNIK
DEPT. OF BUILDING TECHNOLOGY AND STRUCTURAL ENGINEERING
AALBORG UNIVERSITET • AUC • AALBORG • DANMARK

FRACTURE & DYNAMICS
PAPER NO. 60

P. H. KIRKEGAARD, J. C. ASMUSSEN, P. ANDERSEN & R. BRINCKER
AN EXPERIMENTAL STUDY OF AN OFFSHORE PLATFORM
DECEMBER 1994 ISSN 0902-7513 R9441

The FRACTURE AND DYNAMICS papers are issued for early dissemination of research results from the Structural Fracture and Dynamics Group at the Department of Building Technology and Structural Engineering, University of Aalborg. These papers are generally submitted to scientific meetings, conferences or journals and should therefore not be widely distributed. Whenever possible reference should be given to the final publications (proceedings, journals, etc.) and not to the Fracture and Dynamics papers.

INSTITUTTET FOR BYGNINGSTEKNIK
DEPT. OF BUILDING TECHNOLOGY AND STRUCTURAL ENGINEERING
AALBORG UNIVERSITET • AUC • AALBORG • DANMARK

FRACTURE & DYNAMICS
PAPER NO. 60

P. H. KIRKEGAARD, J. C. ASMUSSEN, P. ANDERSEN & R. BRINCKER
AN EXPERIMENTAL STUDY OF AN OFFSHORE PLATFORM

DECEMBER 1994 ISSN 0902-7513 R9441

An Experimental Study of an Offshore Platform

P.H. Kirkegaard, J.C. Asmussen, P. Andersen & R. Brincker

Department of Building Technology and Structural Engineering
Aalborg University
Sohngaardsholmsvej 57, 9000 Aalborg, Denmark

Contents

SUMMARY

This report describes the results of an analysis of the ambient response data collected from a Venezuelian near-shore offshore platform constructed in 1992. Recording of the data have been constantly done during the periode from May 1993 to July 1994. Using these data the structural integrity of the multi-pile offshore platform is investigated by using a vibration based damage detection scheme. Changes in structural integrity are assumed to be reflected in the modal parameters estimated from only output data using an Auto-Regressive Moving Average (ARMA) model. Before the calibration of the ARMA model the quality of the measured data have been investigated. The estimated modal parameters and their corresponding variances are used as input to a probability based damage indicator. This indicator indicates, that since the construction of the platform, minor structural changes have taken place.

PREFACE

The present report *An Experimental Study of an Offshore Platform* has been prepared as a part of the research project *Damage Detection in Structures under Random Loading* which has been performed at the Department of Building Technology and Structural Engineering, Aalborg University.
The authors wish to acknowledge INTERVEP S.A, Research Centre for the Venezuelian Oil Industri, for their kind release of information and data.
Finally, financial support from the Danish Council for Scientific and Industrial Research is gratefully acknowledged.

Rune Brincker
Palle Andersen
John Christian Asmussen
Poul Henning Kirkegaard

Aalborg, Denmark
December, 1994

1 INTRODUCTION

Offshore structures continuously accumulate damage during their service life due to environmental forces such as waves, winds, current and seismic actions. A damage may alter the stiffness and change the modal properties of the structural system, such as natural frequencies, damping ratios and mode shapes. Therefore, much research has been done with respect to structural diagnosis (health monitoring) by measuring vibrational signals of civil engineering structures. The main impetus for doing vibrational based inspection (VBI) is caused by a wish to establish an alternative damage assessment method to the more traditional ones. The most common of the traditional methods is visual inspection. However, damage assessment by visual inspection can be costly, risky and difficult when civil engineering structures such as offshore structures are considered. Besides, a reduction of inspection cost a capable VBI technique can lead to lesser risky and quicker means of assessing structural damage. Many research projects have concluded that it is possible to detect damages in civil engineering structures by VBI, and some techniques to locate damages in civil engineering structures have also been proposed. However, much of the performed research has been based on numerical simulations and/or laboratory models. A throughout review of VBI techniques can be found in Rytter [1]. The idea of using VBI on offshore structures has been developed since the early seventies, see e.g. Loland et al. [2], Campbell et al. [3], Coppolino et al. [4], Haugland et al. [5], Jensen [6], Roitman [7], Hamamonto et al. [8] and Li [9].
In order to use VBI techniques it is necessary to be able to obtain reliable estimates of the dynamic characteristics, e.g. natural frequencies. The estimation may be carried out in the frequency domain or in the time domain. Historically, parameter estimation based on frequency domain models seemed to dominate the theory and practice of the system identification up to the sixties. Since the end of the sixties the interest in the system identification based on time domain models has increased, and now literature on system identification is very much dominated by time domain methods. Often the intended use of the model as well as accuracy requirements on parameter estimates motivates the use of a time domain model and corresponding system identification procedure. In Ljung [10] and Söderström et al. [11] the basic features of system identification based on time and frequency domain approaches are highlighted. For many years the identification techniques based on ARMA models in the time domain have attracted limited interest concerning structural engineering applications. A factor contributing to this situation is that ARMA models have been developed primarily by control engineers and applied mathematicians. Further, ARMA models have been primarily developed concerning systems for which limited a priori knowledge is available, whereas the identification of structural systems relies heavily on understanding of physical concepts. However, in recent years the application of ARMA models to the description of structural systems has become more common, see e.g. Gersch et al. [12] Pandit et al. [13], Hac et al. [14], Kozin et al. [15], Jensen [6], Safak [16], Hamamonton et

al. [8] and Li et al. [9]. The structural time domain identification techniques using ARMA representation have been compared with frequency domain techniques in e.g. Davies et al. [17]. In this and other papers it has been documented that these ARMA time domain modelling approaches are superior to Fourier approaches for the identification of structural systems. These foundings make identification techniques utilizing ARMA algorithms interesting for modal parameter estimation. Especially, with respect to damage detection where modal parameters are used as damage indicators. If modal parameters are used as damage indicators it is important to be able to obtain unbiased estimates. Further, one also want to be able to quantify the uncertainty of the parameters, so conclusions about changes in parameters caused of possible structural changes can be done. This problem can be partially solved by using ARMA models in the time domain.
The aim the present report is to investigate the possibility of detecting changes of the structural integrity of an offshore structure. The structural integrity has been assumed to be reflected in the modal parameters estimated by using full-scale measurements based on natural excitation. The parameter estimation is solved by using a time domain identification method (ARMA). In chapter 2 and 3 the multipile offshore structure and the measured data are described, respectively. Chapter 4 deals with the foundation of the ARMA-model while in chapter 5 the results of the system identifcation are given.

2 DESCRIPTION OF PLATFORM AND INSTRUMENTATION

In the chapter a short description of the considered offshore structure is given.

2.1 Description of Platform

The considered offshore platform built in 1992 is a 58 m long by 20 m wide multipile structure of reinforced concrete holding a steel superstructure which supports the power generation equipment for a large oil production complex. The elevation of the offshore structure in the longitudinal and the transversal direction are shown in figure 1 and 2, respectively. Water depth at the location of the offshore platform is about 30 m. Wave heights in this zone have been reported between 1.2 m and 2.5 m in the longitudinal direction of the platform with recurrence periods of 3.8 and 4.9 s, respectively. The information reported for current action near the platform shows values in the order of 1.4 m/s in the direction of the waves. This platform is very flexible and it experiences continuous vibrations caused by wave and current actions. The platform has been constructed with less number of piles and a different distribution from other offshore platforms built up to 1992. The reinforced concrete base structure is supported by 42 pre-stressed circular piles, 0.9 m in diameter.

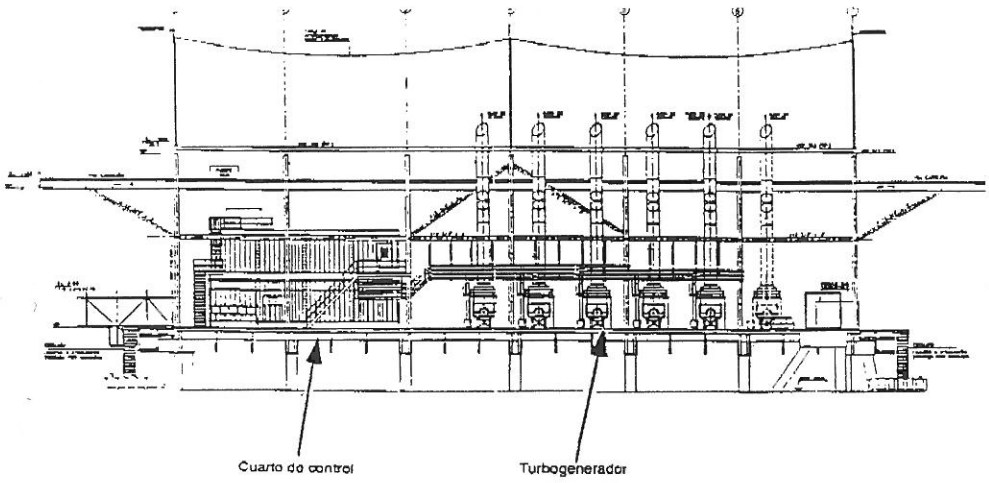

Figure 1: *Elevation of multi-pile offshore structure (longitudinal)*

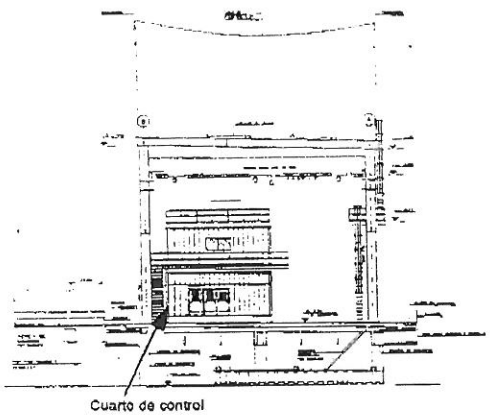

Figure 2: *Elevation of multi-pile offshore structure (transversal)*

2.2 Instrumentation of Platform

The offshore platform was instrumented with three accelerometers, see figure 3, measuring the acceleration response in the longitudinal, transversal and vertical direction, respectively. 160 time-series acceleration measurements where performed between 20/5 1993 and 20/7 1994. The length of the records varies between 19 s and 76 s. A1 and A3 are the two horizontal directions and A2 is the vertical direction. The sampling frequency is 200 Hz for all measurements.

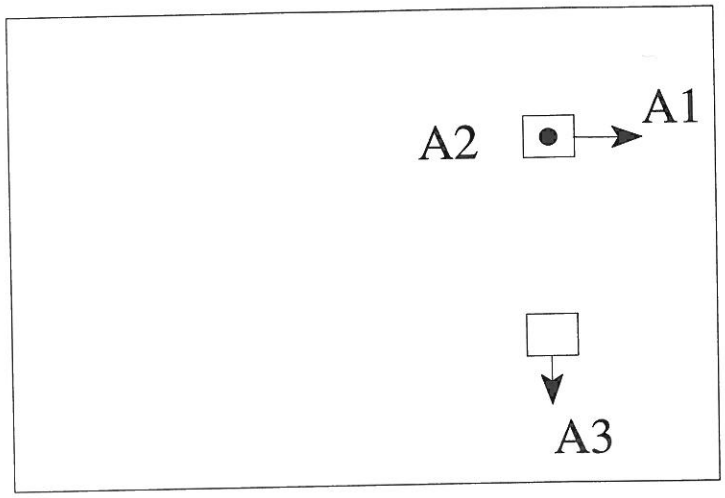

Figure 3: *Location of Accelerometers*

3 DESCRIPTION OF MEASUREMENTS

In this chapter the measurements are presented. Furthermore the assumptions used for system identification in chapter 5 about the recorded time-series are investigated.

3.1 Presentation

Only the response of the platform excited by natural loads such as wind and waves is measured. This is due to the difficulties in measuring the ambient excitation. The number, date, time, duration and the numerical maximal acceleration in the three directions A1, A2 and A3, respectively, are shown in appendix A,table 1-3. There are generally more noise present in the measurements in the A1 direction than the

A3 direction. Furthermore some of the measurments shows that the acceleration is constant in time, except for an impulse. Figure 4 a) shows a typical time-series in the A1 direction and b) a time-series unuseable for system identification.

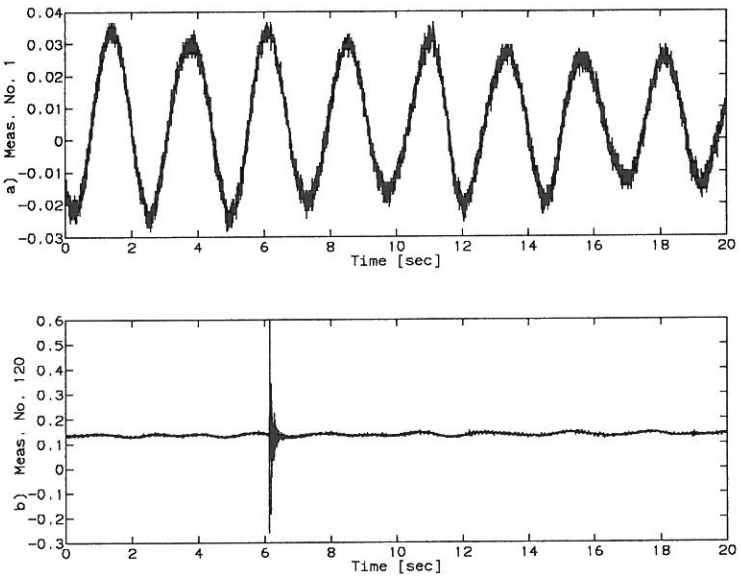

Figure 4: *Typical time-series a) and time-series unuseable for system identification b). A1 direction.*

Time-series like figure 4 b) is marked with '-' in table 1-3. This is valid for all three directions. The measurements of the acceleration in the A2 direction are generally dominated by a higher frequency than measurements in the A1 and A3 direction. In figure 5 a proper time-series and a time- series equivalent with figure 4 b) are shown.

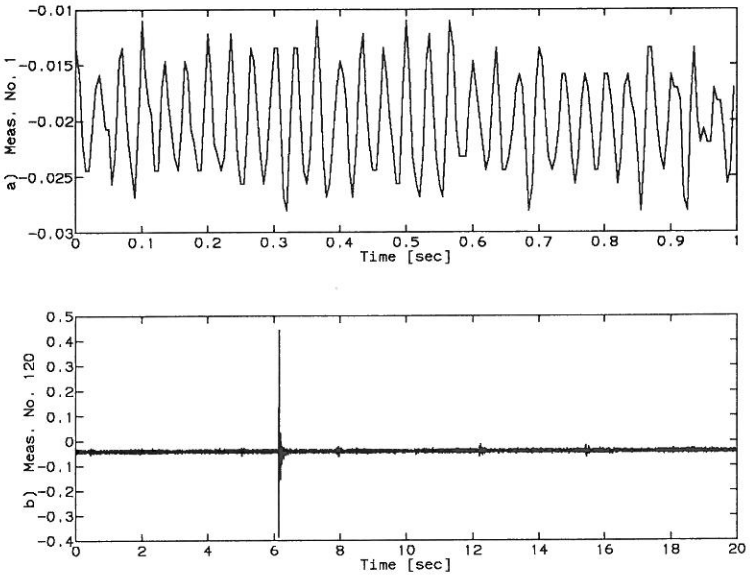

Figure 5: *Typical time-series a) and time-series unuseable for system identification b). A2 direction.*

In figure 6 time-series for the A3 direction are shown.

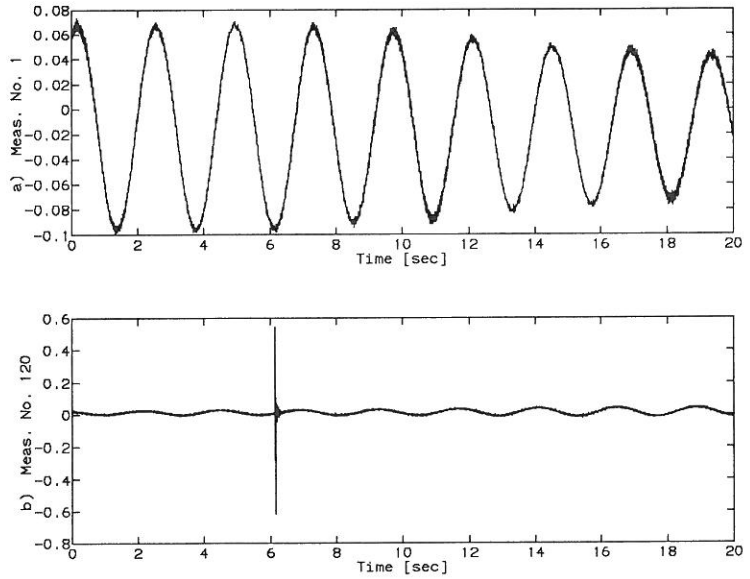

Figure 6: *Typical time-series a) and time-series unuseable for system identification b). A2 direction.*

A Comparison of figure 6 a) with figure 4 a) shows that there are more noise present in measurements in the A1 direction than the A3 direction. This is valid in general for all recorded time-series.

The power spectral densities for the three typical timeseries (figure 4-6) are shown in figure 7-9

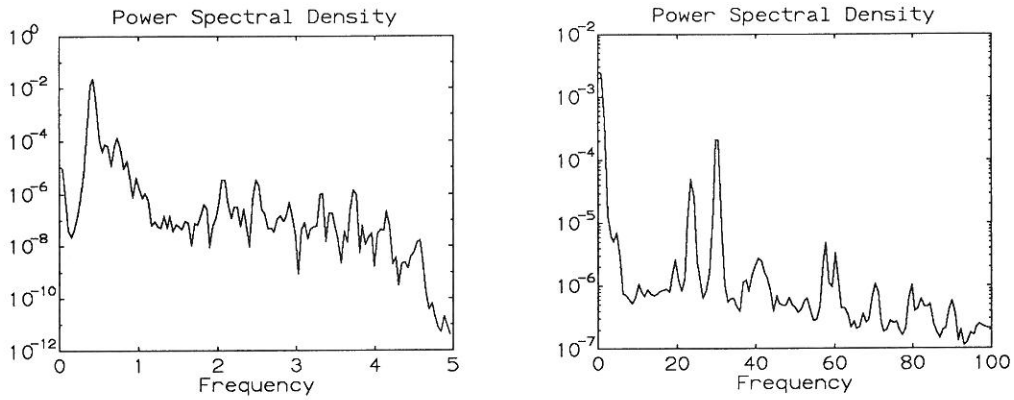

Figure 7: *Power spectral density. A1 direction.*

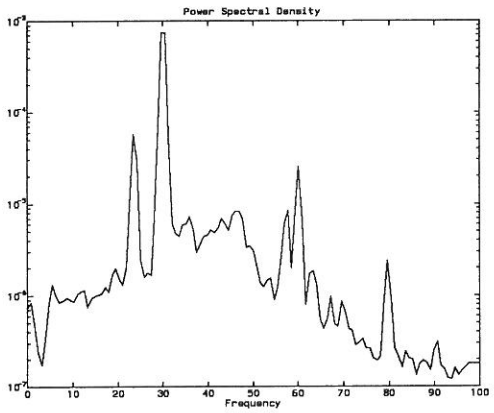

Figure 8: *Power spectral density. A2 direction.*

It is concluded that using the measeruments in the A3 direction will be a better input for system identification, than the measurements in the A1 direction. This is

due to the fact that measurements in the A3 direction are less noisy which is seen from figure 4.a and 7.a.

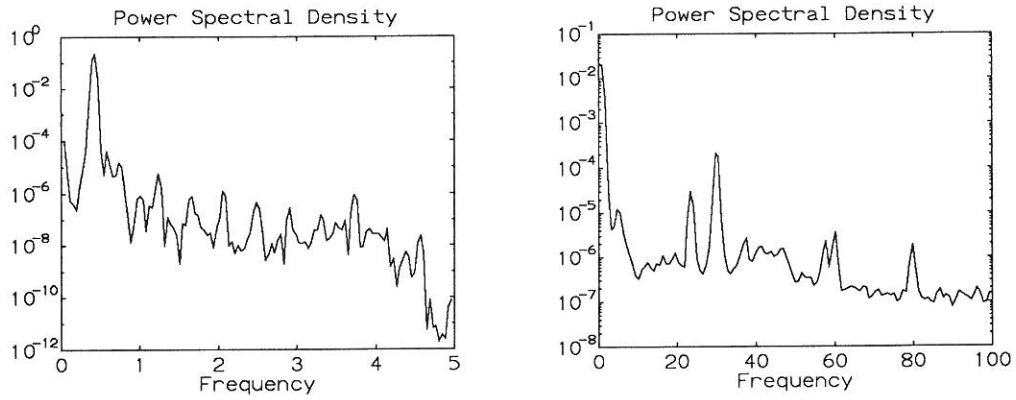

Figure 9: *Power spectral density. A3 direction.*

3.2 Investigation of Assumption

In chapter 5 the system identification will be carried out. The assumptions are that the time series are realizations of a stationary zero-mean Gaussian process. Theoretically this will be true if the structure can be described by a linear second order differential equation excited by a stationary zero-mean Gaussian process. This implies that the time-series should be investigated for Gaussianity and stationarity. To investigate the time-series for Gaussianity the mean, standard deviation, skewness and kurtosis are calculated and shown for all the recorded time-series in table 4-9. From table 4-9 it is seen that the time-series are not zero mean processes. This can be due to the calibration of the instrumentation. It will be assumed that this is the reason and the time series used in further investigations are normalized to be zero mean processes.
If the time-series are Gaussian processes the skewness and kurtosis theoretically are 0 and 3. Comparing this with the values of table 4-9, it is seen that that the values of skewness and kurtosis are only approximately those of a Gaussian process. Another way to investigate for Gaussianity is to make a probability plot

of the time-series. This is done in figure 10-12 for the first measurements in all three directions. The standard deviation is nomalized to one.

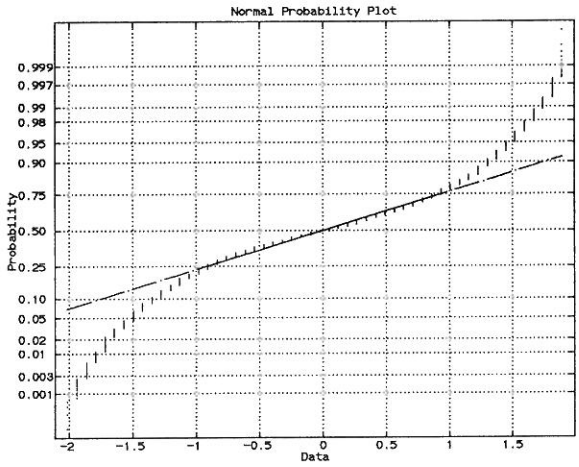

Figure 10: *Normal probability plot for measurement no. 1 in the A1 direction.*

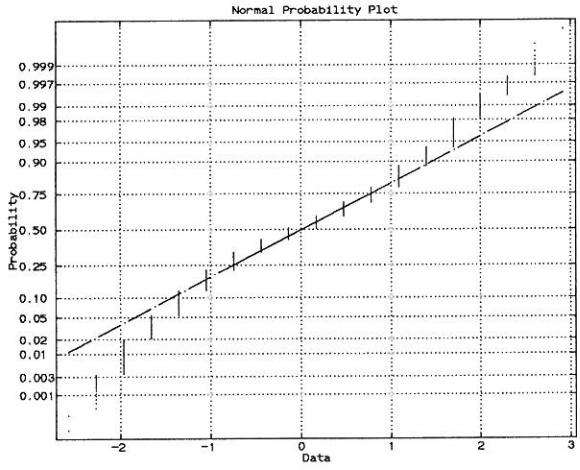

Figure 11: *Normal probability plot for measurement no. 1 in the A2 direction.*

The figures 10-12 shows that in the tales the time-series differs from the normal distribution. This can be explained by the short duration of the time-series. What is more interesting is that especially for measurements in the A1 and A2 direction there are only very few different values in the measurements. An explanation could be that the calibration of the A/D-converter has been poor. Therefore system identification based on measurements in the A1 and A2 direction can be very uncertain.

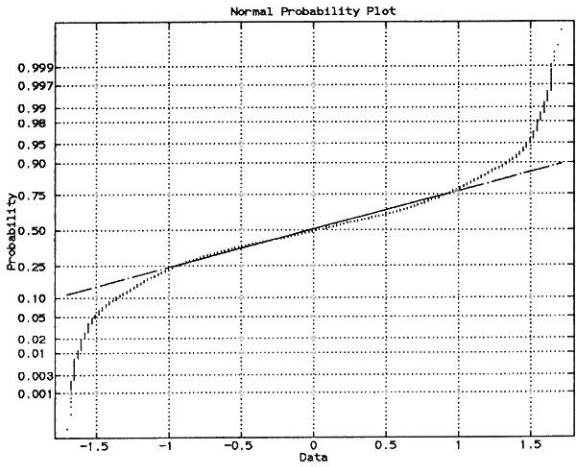

Figure 12: *Normal probability plot for measurement no. 1 in the A3 direction.*

4 ANALYSIS OF MEASUREMENTS

This chapter deals with the foundation of the ARMA model used in chapter 5 for system identification of the offshore structure.

4.1 Description of ARMA models

An Auto-Regressive-Moving-Average ARMA(n, m) model of order n, m describing the response at the discrete time points y_t is given by

$$y_t = \sum_{i=1}^{n} \Phi_i y_{t-i} - \sum_{i=1}^{m} \mathcal{O}_i e_{t-i} + e_t \tag{4.1}$$

Φ_i is an Auto Regressive (AR) parameter, $\mathcal{O}_i$ is the Moving Average (MA) parameter and e_t is a time series of a white noise process. This model involves a difference equation in which the output of the system is expressed as a linear combination of past output, as well as present and past input. This kind of model is particular well suited for identification and response calculation purposes since they provide efficient system representations.
If an ARMA$(2n, 2n-1)$ model is used for a stationary Gaussian white noise excited linear n-degrees-of-freedom system it can be shown that the covariance of the response due to the ARMA-model and that of the white noise excited structure will be identical, see e.g. Kozin et al. [15]. In other words, an ARMA model will provide an unbiased estimate of the autospectrum provided the assumptions hold. It is seen that the parameter identification of civil engineering structures by using an ARMA model assumes that the response data are caused by a white noise input to the structure. However, for wave or wind excited lightly damped civil engineering

structures, this assumption will normally hold, see e.g. Morgan et al. [18], Jensen [6] and Srinavasan [19].
The AR and MA parameters are obtained by minimizing an error function V_N expressing the variance of e_t

$$V_N = \frac{1}{N}\sum_{t=1}^{N}\epsilon_t^2 = \frac{1}{N}\sum_{t=1}^{N}\frac{1}{2}(y_t^M - \hat{y}_t)^2 \tag{4.2}$$

where N is the number of data and ϵ_t is the prediction error. y_t^M and $\hat{y}_t$ are the measured response and the predicted response by (1), respectively. It may be noticed that the white noise assumption must be checked when the AR and MA parameters and the residuals have been estimated. If the assumption does not hold it may indicate that the order of magnitude of the model is too low and therefore should be increased.
When the AR parameters are estimated the $2n$ roots, λ_i of the characteristic polynomial of the AR-parameters are found

$$\lambda^{2n} - \Phi_1\lambda^{2n-1} - \cdots - \Phi_{2n-1}\lambda - \Phi_{2n} = 0 \tag{4.3}$$

In e.g. Pandit et al. [13] it is shown that the roots are related to the modal parameters through the $2n$ relations

$$\lambda_i = \exp(\mu_i \Delta t) \qquad i = 1, 2, .., 2n \tag{4.4}$$

where Δt is the sampling interval. μ_i has the following relation to the modal parameters for an underdamped system

$$\mu_i = -\omega_i\zeta_i \pm i\omega_i\sqrt{1-\zeta_i^2} \qquad \zeta_i < 1.0 \tag{4.5}$$

By using the ARMA model all the information in the measured time series is used to estimate the AR-parameters. This implies that a large amount of data has to be handled in the system identification process implying that it can be time consuming to estimate the parameters. Especially, when the model order increases, caused of the non-linear optimization which has to be used to get the AR-parameters and the MA-parameters. However, Pandit et al. [13] has shown that any ARMA model can be represented by an AR model if the model order is chosen sufficiently high. This implies that the AR-parameters can be estimated directly by linear regression obtaining at least squares fit between the measured time series and the AR-model.

4.2 Model Selection and Model Validation

Model selection involves the selection of the form and the order of the ARMA model, and constitutes the most important part of the system identification. Model validation is to confirm that the model estimated is a realistic approximation of the actual system. A throughout description of the problem of model selection and validation is given in e.g. Ljung [10] and Söderström [11]. In the following it will be shortly explained how one can deal with this problem. In general, the choice of the model structure involves:

• *Model type.* This involves the selection between non- linear and linear models, between black-box and physical models etc..

• *Model size.* I.e. choice of model order and number of adjustable parameters.

• *Model parametrization.* I.e. the way in which the number of parameters enter into the model.

The choice of the model to a large extent should be made according to the aim of the final purpose. There is no general solution of this problem but a large number of methods to assist in the choice of an appropriate model structure exists. These methods can be divided into several categories. They are based on

• *A priori knowledge.* Information about the system obtained from e.g. understanding of the physics of the system, design calculations, etc.

• *Preliminary data analysis.* Extracting information from the data that involve determination of a complete model of the system. E.g. spectral analysis estimates will give valuable information about resonance peaks. Further, a preliminary data analysis test for non-linear effects can be performed.

• *Comparison of model structures.* A most natural approach to search for a suitable model structure is simply to test a number of different ones and then to compare the resulting models. However, it is usually only feasible to do this with simple models because of the amount of calculation involved in more complicated models.

For such comparisons, as mentioned above a discriminating criterion is needed. The comparison of the model structures can be interpreted as a test for a significant decrease in the minimal values of the loss function V_N associated with the model structures in question. As a model structure is expanded, e.g. increasing the number of adjustable parameters, the minimal value of V_N decreases since new degrees of freedom have been added to the optimization problem. The decrease of V_N is a consequence that more flexible model structures give a possibility for better fit to the data. On the other hand when a good fit can be obtained there is no reason to increase e.g. the number of adjustable parameters. An overparameterized model structure, i.e. containing several models giving a perfect description of the actual system, can lead to unnecessarily complicated computations for finding the parameter estimates. An underparameterized model, i.e. a model having to few parameters to describe the system adequately, may be inaccurate. In order to deal with this problem Akaike, see Akaike [20], suggested a Final Prediction Error (FPE) criterion and a closely related Information Theoretic Criterion (AIC) of the type

$$FPE = \frac{1 + \frac{n}{N}}{1 - \frac{n}{N}} V_N \tag{4.6}$$

$$AIC = \log[(1 + \frac{2n}{N}) V_N] \tag{4.7}$$

where N is the length of the data record and n is the total number of estimated parameters. The model structure giving the smallest value of these criteria is selected. The AIC and FPE criteria penalize using too high model orders, i.e. their value may increase with increasing model order.
In e.g. Ljung [10] and Söderström [11] other approaches to model structure comparisons are given.

Model validation is the final stage of the system identification procedure. In fact model validation overlaps with model structure selection. Since system identification is an iterative process various stages will not be separated: models are estimated and the validation results will lead to new models etc.
Model validation involves two basic questions:

- What is the best model within the chosen model structure ?
- Is the model fit for its purpose ?

One of the dilemmas in model validation is that there are many different ways to determine and compare the quality of the estimated models. First of all, the subjective judgement in model validation should be stressed. It is the user that makes the decision based on numerical indicators. The variance of the parameter estimates can be such an indicator. High values indicate a model with a bad fit or overparameterization. It is also important to check whether the model is a good fit for the data recording to which it was estimated. If it is a bad fit it may e.g. indicate that the model represents a local minimum. Simulation of the system with the actual input and comparing the measured output with the simulated model output can also be used for model validation. Statistical tests of the prediction errors ϵ_t are also typically used numerical indicators for model validation. If the statistical distribution of ϵ_t matches the assumed distribution then it can be concluded that the system dynamics is indeed well represented by the model. Any different trend in the statistical characteristics originally assumed is an indication that either the model or the noise is incorrectly assumed or that the parameters are incorrectly estimated.
The above-mentioned tools for model validation lead to a conclusion as to whether the model is fit for its purpose.

4.3 Estimation of Parameter Uncertainty

From measurements of the response process it is possible to get unbiased estimates of the AR-parameters Φ_i see e.g. Pandit et al. [13], where estimates of the variances of the estimated parameters can be estimated by the Cramer-Rao lower bound. This implies that the covariance matrix of parameter estimates can be obtained by the inverse of the Fisher information matrix $\overline{\overline{J}}$ which can be written

$$\overline{\overline{J}} = \frac{N}{\lambda_\mathcal{E}} E[\overline{\Psi}_t(\overline{\Phi})^T \overline{\Psi}_t(\overline{\Phi})] \tag{4.8}$$

A realization of the stochastic process $\{\overline{\Psi}_t(\overline{\Phi})\}$is given by

$$\overline{\psi}_t(\overline{\Phi}) = \frac{\partial \epsilon_t(\overline{\Phi})}{\partial \overline{\Phi}} \tag{4.9}$$

It is assumed that the variance $\lambda_\mathcal{E}$ of the prediction error process $\{\mathcal{E}_t\}$ is V_N. $\overline{\Phi}$ is a vector including the AR-parameters.
When the elements of the information matrix are calculated the parameter covariance matrix $\overline{\overline{C}}_{\hat{\overline{\theta}}_N}$ of estimates of the parameter vector $\hat{\overline{\theta}}_N$ can be expressed in the following way

$$\overline{\overline{C}}_{\hat{\overline{\theta}}_N} \approx \overline{\overline{A}}\,\overline{\overline{J}}^{-1}\overline{\overline{A}}^T \tag{4.10}$$

where the transformation matrix $\overline{\overline{A}}$ is given by

$$\overline{\overline{A}} = \begin{bmatrix} \frac{\partial f_1}{\partial \Phi_1} & \frac{\partial f_1}{\partial \Phi_2} & \cdot & \cdot & \cdot & \cdot & \cdot & \frac{\partial f_1}{\partial \Phi_{2n}} \\ \frac{\partial \zeta_1}{\partial \Phi_1} & \frac{\partial \zeta_1}{\partial \Phi_2} & \cdot & \cdot & \cdot & \cdot & \cdot & \frac{\partial \zeta_1}{\partial \Phi_{2n}} \\ \cdot & \cdot & \cdot & \cdot & \cdot & \cdot & \cdot & \cdot \\ \cdot & \cdot & \cdot & \cdot & \cdot & \cdot & \cdot & \frac{\partial f_n}{\partial \Phi_{2n}} \\ \cdot & \cdot & \cdot & \cdot & \cdot & \cdot & \cdot & \frac{\partial \zeta_n}{\partial \Phi_{2n}} \end{bmatrix} \tag{4.11}$$

$\hat{\overline{\theta}}_N$ is an estimator of the parameter vector $\overline{\theta} = [f_1, \zeta_1, f_2, \zeta_2, ..., f_n, \zeta_n]^T$. The above estimation of $\overline{\overline{A}}$ will only be accurate if the function is sufficiently smooth since it corresponds to a linear approximation of the function describing the inverse transformation from AR- parameters to the parameters $\overline{\theta}$, see e.g. Kirkegaard [21].

5 RESULTS

This chapter presents the results of the system identification. Further, the structural integrity of the multi-pile offshore platform is investigated by using the estimated modal parameters and their corresponding variances as input to a probability based damage indicator. It was decided to limite the identification to the first two modes, one in the longitudinal and one in the transversal direction.

5.1 Data Acquistion and Signal Processing

Since the number of points of the records were too short for identification using an ARMA-model, records from the same day were combined into one time series. This reduces the number of time series to 29. The discontinuities between the individual data segments were smoothed by use of a tapering function (a half Hanning Window). In order to improve the precision of the identification the signals were

detrended and outliers were removed. Since the expected highest frequency in the structure is much smaller than the Nyquist frequency, the sampling rate was decreased by decimating the records in order to reduce the noise effects. The new sampling rate after decimation was 10 Hz. Before the decimation the record was low-pass filtered beyond the new Nyquist frequency.

5.2 Selection and Validation of ARMA-model

In the following it is explained how the ARMA-model was selected and validated. The results are given for a recorded signal in the longitudinal direction.
By incorporating the FPE and AIC criteria it was determined that a 4 degrees of freedom model was appropriate. I.e. a 8th-order model giving an ARMA(8,7).
Figure 13 shows a plot of the poles (x) and zeros (o) and it is seen that all the poles and zeros are inside the unit circle in the complex plane. The poles and zeros are given with confidence regions corresponding to three standard deviations. If these regions overlap a lower model order should have been tried, since this is a result of a near pole-zero cancellation in the dynamic model indicating that the model order is too high. The most dominant mode of the system is the one corresponding to the pole closest to the unit circle.

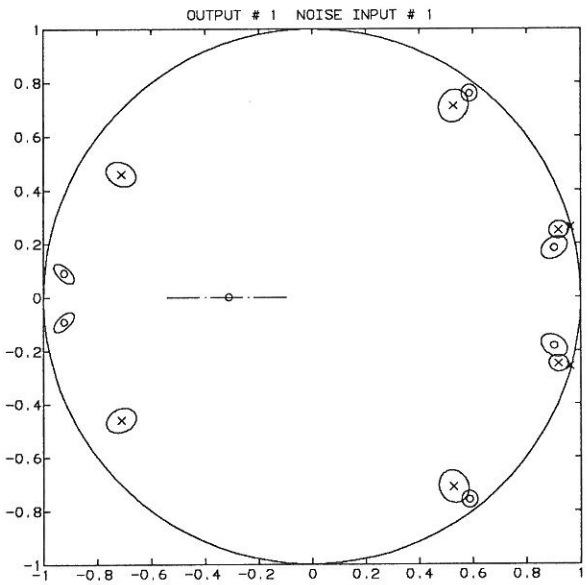

Figure 13: *Pole-Zero plot.*

As discussed in chapter 4.2, after the model is selected and the parameters are determined, the next step is to check the validity of the model. The match of

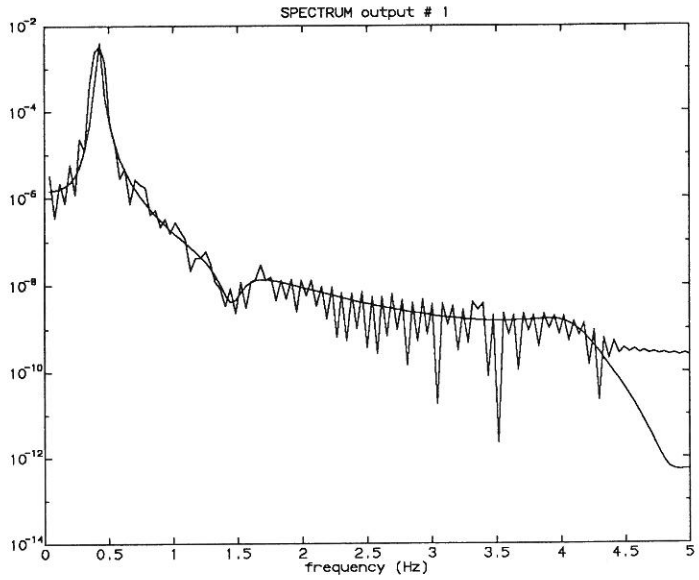

Figure 14: *Comparison of direct estimated spectrum and spectrum obtained from the ARMA-model (full-line).*

the power spectrum obtained by a Fast Fourier Transformation and the spectrum obtained from the ARMA-model are shown in figure 14. The figure shows a good match. Next the residuals of the identification are checked. Residuals are defined as the difference between the model output and the recorded output signal. In order to have a valid identification, the residuals should be a white-noise sequence. The plot of the spectrum and autocorrelation of the residual time series are given in figure 15 and figure 16, respectively.

Visual inspection of the autocorrelation and spectrum of the residual time series in figure 15 and figure 16, respectively, suggests that the residuals are close to a white-noise sequence, since the peaks are distributed in all frequencies. A more accurate check is to test the autocorrelation of the residuals. Two straight lines in the figure show the 99% confidence level. For model validity, i.e. whiteness of residuals, the autocorrelation should not exceed these levels, except at zero lag. Figure 15 shows that the autocorrelation remains, for the most part, within the limits, and therefore validate the model. The autocorrelation test shows if there is any correlation in the residuals. In an ideal identification the residuals would be identical to a white-noise sequence.
As a final test for model validity, a comparison of model output with recorded output. This is a more strict test than the previous ones. However, figure 16 shows that the match is fairly good. Based on all the above checks, it can be concluded that the estimated ARMA-model for the offshore structure is satisfactory.

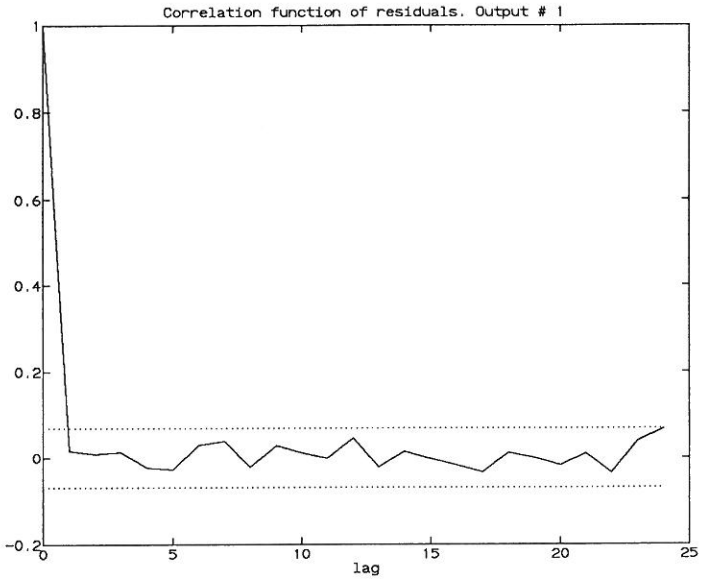

Figure 15: *Autocorrelation of the residual time series.*

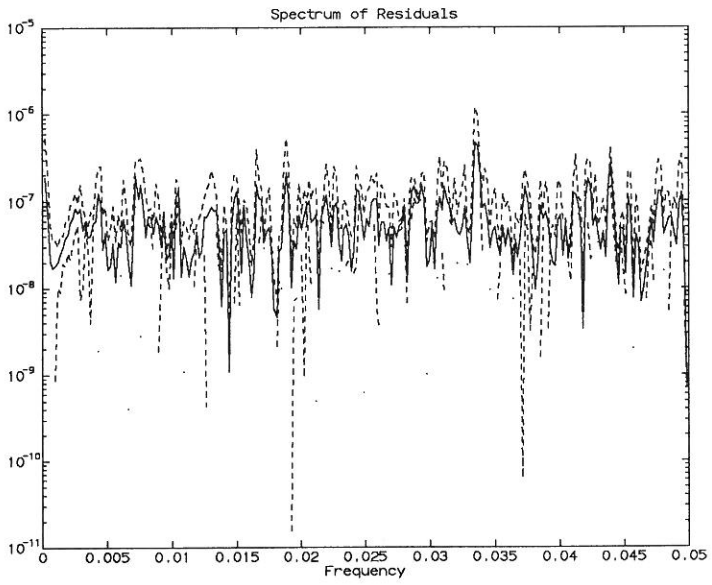

Figure 16: *Spectrum of the residual time series.*

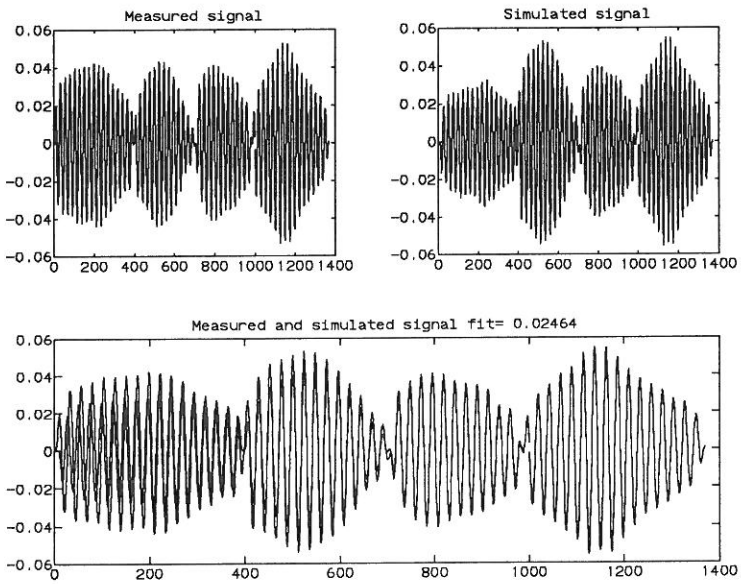

Figure 17: *Comparison of calculated accelerations with recorded accelerations, plotted separately and together.*

5.3 System Identification Results

In this chapter the estimated natural frequencies for the first and second mode, respectively, are presented and discussed. The first and second natural frequencies were estimated as approximately 0.42 s and 0.62 s, respectively, which correspond to the values obtained from FEM calculations, see Tallavó et al. [24]. In figure 18 the estimates of the first and second natural frequencies, respectively, are shown as a function of time. The uncertainty given as plus minus three times the standard deviation is shown with the dotted lines. As it should be expected from the spectrum f_2 seems to be more uncertain than f_1. Further, it is seen that f_2 has a small decrease. However, figure 18 does not show wether these changes are significant. Assuming f_i to be independent Gaussian distributed variables standard theory gives that the probability of negative changes $P_{\Delta f_i}$ in f_i is given by

$$P_{\Delta f_i} = \Phi\left(\frac{f_{i0} - f_i}{\sqrt{\sigma_i^2 + \sigma_{i0}^2}}\right) \tag{4.12}$$

where Φ is the unit normal distribution function and σ_i^2 is the variance of f_i. σ_{i0}^2 is the variance of the frequency f_{i0} of the assumed undamaged structure, i.e. the first estimated frequency. A negative change in f_i is assumed to indicate that the structure has suffered structural changes.
Figure 19 shows the probability of negative change in f_1 and f_2, respectively as a function of time. It is seen that the two curves have many fluctuations perhaps due to the fact that the estimates of the two frequencies and their variances are only

based on short time series. This implies that the estimates are uncertain. However, it is seen in figure 19 that a change has occurred in the first and second frequency with 70 and more than 90 % probability, respectively. This means that with a probability close to one the structural properties have changed during the first 12 months of the operation. If the structure has changed however, the changes are small and might be due to cracking of the concrete base structure or changes in the foundation that do not affect structural safety. The analysis of the dynamical responses indicates the usefullness of further investigations.

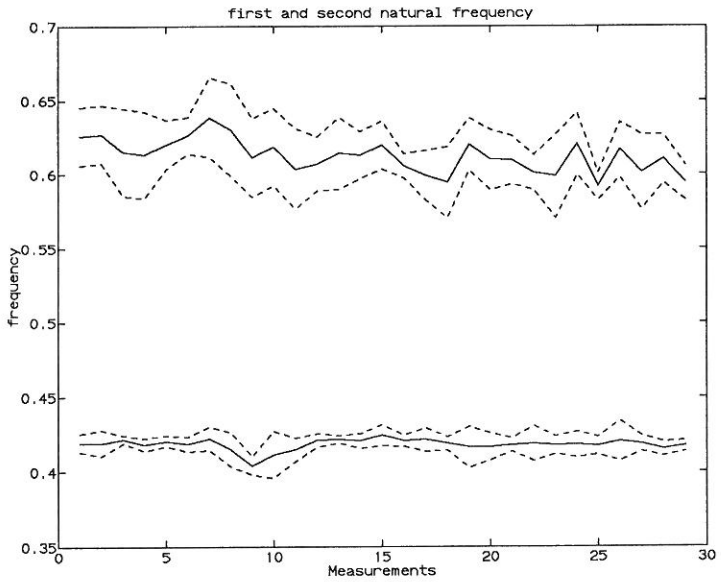

Figure 18: *First and second natural frequencies as function of time.*

6 CONCLUSIONS

In this report the structural integrity of a multi-pile offshore platform is investigated by using a vibration based damage detection scheme. Changes in structural integrity are assumed to be reflected in the modal parameters estimated from only output data using an Auto-Regressive Moving Average (ARMA) model. A damage indicator given as the probability of negative changes in the first two natural frequencies is used to investigate the integrity of the structure. Based on this damage indicator it is concluded that with a probability close to one the considered offshore structure has suffered structural changes in the first year of operation. The changes are small however, and their influence on structural safety must be clarified by further investigations.

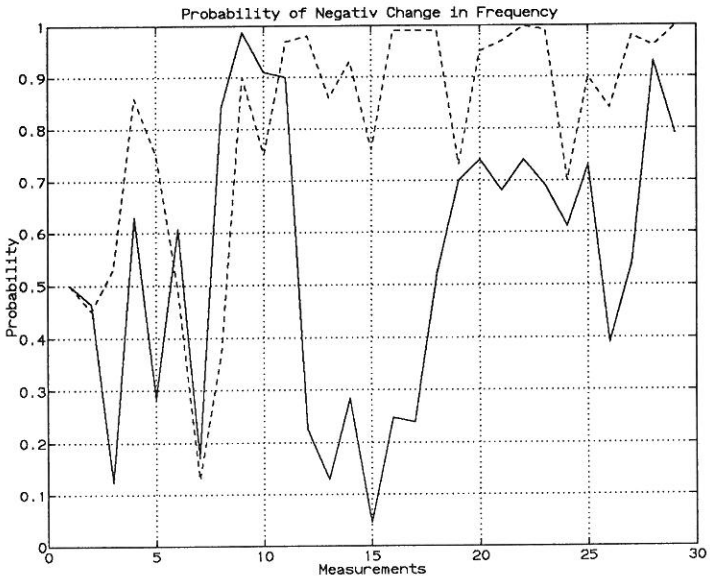

Figure 19: *Damage indicator $P_{\Delta f_i}$ as function of time.*

References

[1] Rytter, A.: *Vibration Based Inspection of Civil Engineering Structures.* Ph.D thesis, Aalborg University, 1993.

[2] Loland, O. & C.J. Dodds: *Experiences in Development and Operating Integrity Monitoring Systems in the North Sea.* Offshore Technology Conference, Paper 2551, Houston, 1975.

[3] Campbell, R.B. & J.K. Vandiver: *The Estimation of Natural Frequencies and Damping Ratios of Offshore Structures.* Offshore Technology Conference, Paper 3861, 1980.

[4] Copolino, R.N. & S. Rubin: *Detectability of Structural Failures in Offshore Platforms by Ambient Vibration Monitoring.* Offshore Technology Conference, Paper 3865, 1980.

[5] Haugland, H. & S.L. Yaas: *Underwater Detection and Monitoring of Fatigue Cracks on a Dynamic Loaded K-node with Internal Stiffeners.* Offshore Technology Conference, Paper 5869, 1988.

[6] Jensen, J. L.: *System Identification of Offshore Platforms.* Ph.D thesis, Aalborg University, 1990.

[7] Roitman, N, P.F. Viero, C. Magluta, R.C. Batista & L.F. Rosa: *Identification of Offshore Structural Damage using Modal Analysis Techniques.* Mechanical Systems and Signal Processing, Vol. 6, No. 3, 1992.

[8] Hamamonto, T. & I. Kondo: *Preliminary Experiment for Damage Detection of Offshore Structures.* Proc. of the Third Int. Offshore and Polar Engineering Conference, Singapore, 1993.

[9] Li, C.-S., R.-J. Shyu, W.-J. Ko & H.-T. Lin: *Multichannel Vibration Time Series Analysis of an Offshore Structural Model.* J. CSME, Vol. 14, No. 1, 1993.

[10] Ljung, L.: *System Identification: Theory for the User.* Prentice Hall, Englewood Cliffs, 1987.

[11] Söderström, T. & P. Stoica: *System Identification.* Prentice Hall, 1987.

[12] Gersch, W. & R. Liu: *Time Series Methods for the Synthesis of Random Vibration Systems.* ASME Transactions, Journal of Applied Mechanics, Vol. 98, No. 2, 1976.

[13] Pandit, S. W. & N. P. Metha: *Data Dependent Systems Approach to Modal Analysis Via State Space.* ASME paper No. 85-WA/DSC-1, 1985.

[14] Hac, A. & P. Spanos: *Time Domain Structural Parameters Identification.* Proc. of the Session of Structural Congress 87 (J. M. Roesset, ed.), 1987.

[15] F. Kozin & H. G. Natke: *System Identification Techniques.* Structural Safety, Vol. 3, 1986.

[16] Safak, E. : *Identification of Linear Structures using Discrete-Time Filters.* Journal of Structural Engineering, Vol. 117, No. 10, 1991.

[17] Davies, P., & J. K. Hammond: *A Comparison of Fourier and Parametric Methods for Structural System Identification.* Journal of Vibration, Acoustics, Stress and Reliability in Design. Vol. 106, pp.40-48, 1984.

[18] Morgan, B. J., S. C. Larson & R. G. Oesterle: *Field Measured Dynamic Characteristics of Buildings.* Proc. of the Sessions of Structures Congress 87,(D. R. Sherman, ed.), 1987.

[19] Srinavasan, M. G., C. A. Kot & B. J. Hsieh: *Dynamic Testing of As-Built Structures - A Review and Evaluation.* NUREG/CR-3649, ANL-83-20, U.S. Nuclear Regulatory Commission, Washington, D. C., 1984.

[20] Akaike, H.: *Fitting Autoregressive Models for Prediction.* Am. Inst. Stat. Math., Vol. 21, pp. 243-347, 1969.

[21] Kirkegaard, P.H.: *Optimal Design of Experiments for Parametric Identification of Civil Engineering Structures.* Ph.D-Thesis, Aalborg University 1991.

[22] PC-MATLAB for MS-DOS Personal Computers, The Math Works, Inc., 1989.

[23] Brincker, R., S. Krenk & J. Laigaard Jensen : *Estimation of Correlatioon Functions by the Random Decrement Technique.* Fracture and Mechanics Paper No. 26, Aalborg University, 1990.

[24] Tallavó F., M.E. Martĩnez & D.J. Ewins: *Experimental Evaluation of Vibrations in an Operating Offshore Platform.* Proc. of the 13th International Conference on Modal Analysis, Nashville, 1995.

APPENDIX A: Measurement List

No.	Date	Time	Duration	A1 (%g)	A2 (%g)	A3 (%g)
			[sec]	$[m/s^2]$	$[m/s^2]$	$[m/s^2]$
1	20/05/93	02:14:49	30	0.73	0.61	2.00
2	08/06/93	02:11:55	35	0.54	0.73	1.20
3	08/06/93	02:13:55	33	0.51	0.68	1.27
4	08/06/93	02:19:37	46	0.44	0.68	1.22
5	08/06/93	10:29:16	33	0.54	0.78	1.10
6	09/06/93	05:08:31	40	0.54	0.66	1.25
7	09/06/93	05:12:11	31	0.51	0.66	1.22
8	09/06/93	05:15:05	28	0.46	0.63	1.20
9	09/06/93	09:05:51	38	0.59	0.63	1.42
10	11/06/93	13:06:07	72	0.66	0.73	1.61
11	12/06/93	08:34:24	42	0.54	0.68	1.29
12	12/06/93	10:45:51	78	0.81	0.71	1.66
13	13/06/93	10:01:07	64	0.93	0.83	1.39
14	13/06/93	19:42:22	31	0.76	0.71	1.10
15	14/06/93	19:14:14	31	0.81	0.66	1.07
16	14/06/93	19:22:12	49	0.85	0.68	1.29
17	14/06/93	19:23:35	28	0.76	0.68	1.07
18	14/06/93	19:32:54	28	0.78	0.68	1.07
19	14/06/93	19:42:09	42	0.85	0.66	1.29
20	14/06/93	19:46:33	33	0.81	0.68	1.15
21	14/06/93	19:51:28	32	0.78	0.66	1.12
22	14/06/93	20:25:55	40	0.81	0.68	1.12
23	15/06/93	09:21:23	53	0.88	0.73	1.34
24	15/06/93	09:59:10	51	0.85	0.73	1.42
25	15/06/93	22:03:58	49	0.90	0.63	1.32
26	15/06/93	22:10:29	36	0.85	0.63	1.20
27	15/06/93	22:17:06	51	0.90	0.63	1.15
28	15/06/93	22:19:06	51	0.81	0.63	1.10
29	15/06/93	22:20:06	39	0.88	0.66	1.12
30	15/06/93	22:30:31	31	0.83	0.63	1.12
31	15/06/93	22:31:57	37	0.81	0.63	1.20
32	15/06/93	22:38:11	28	0.81	0.61	1.05
33	17/06/93	08:25:54	41	0.93	0.68	1.15
34	17/06/93	23:21:12	28	0.98	0.66	1.07
35	17/06/93	23:23:10	29	0.93	0.68	1.12
36	18/06/93	22:53:34	31	0.93	0.66	1.03
37	19/06/93	09:50:31	67	0.90	0.76	1.59
38	23/06/93	09:18:41	31	0.76	0.71	1.10
39	23/06/93	10:27:30	29	0.78	0.83	1.07
40	23/06/93	17:59:09	36	0.83	0.56	1.12
41	26/06/93	07:50:02	32	0.85	0.76	1.12
42	26/06/93	07:52:32	35	0.81	0.73	1.20
43	26/06/93	07:53:32	28	0.78	0.73	1.10
44	27/06/93	06:43:53	28	0.78	0.68	1.12
45	27/06/93	06:46:16	28	0.76	0.68	1.20
46	27/06/93	22:30:56	29	0.85	0.63	1.03
47	28/06/93	08:31:09	28	0.81	0.73	1.05
48	28/06/93	08:46:19	28	0.81	0.73	1.10
49	28/06/93	08:58:14	28	0.83	0.73	1.07
50	29/06/93	06:52:21	45	0.78	0.68	1.29

Table 1: *Date, time, duration and numerical maximal acceleration in the three directions*

No.	Date	Time	Duration	A1 (%g)	A2 (%g)	A3 (%g)
			[sec]	$[m/s^2]$	$[m/s^2]$	$[m/s^2]$
51	30/06/93	06:15:57	37	0.81	0.66	1.17
52	30/06/93	06:26:07	52	0.93	0.78	1.27
53	30/06/93	08:00:04	31	0.76	0.71	1.12
54	30/06/93	08:01:40	28	0.81	0.68	1.05
55	01/07/93	09:25:08	28	0.81	0.76	1.05
56	04/07/93	21:11:52	33	0.93	0.66	1.07
57	04/07/93	21:48:44	28	0.95	0.63	1.00
58	05/07/93	05:29:15	59	0.85	0.71	1.17
59	05/07/93	05:31:34	40	0.83	0.66	1.15
60	05/07/93	05:33:36	52	0.81	0.68	1.17
61	05/07/93	05:37:34	49	0.90	0.68	1.27
62	05/07/93	05:43:42	28	0.81	0.68	1.05
63	05/07/93	05:44:06	38	0.83	0.68	1.12
64	05/07/93	05:46:01	76	0.88	0.76	1.29
65	05/07/93	05:47:13	40	0.85	0.71	1.15
66	05/07/93	05:51:53	38	0.88	0.71	1.03
67	05/07/93	05:55:17	38	0.81	0.71	1.22
68	05/07/93	06:28:11	28	0.81	0.71	1.05
69	05/07/93	07:25:32	28	0.88	0.71	1.10
70	05/07/93	07:26:53	28	0.78	0.71	1.05
71	05/07/93	08:13:41	28	0.73	0.76	1.07
72	05/07/93	19:17:32	28	0.78	0.68	0.98
73	06/07/93	11:31:38	45	0.93	0.76	1.29
74	06/07/93	14:41:21	37	0.85	0.76	1.05
75	06/07/93	19:45:56	28	0.98	0.73	1.00
76	06/07/93	19:51:26	28	0.78	0.73	1.03
77	06/07/93	20:00:29	47	0.95	0.76	1.37
78	06/07/93	20:10:18	31	0.83	0.73	1.05
79	06/07/93	20:12:31	19	0.83	0.76	1.05
80	23/08/93	18:55:30	33	1.07	0.66	1.73
81	31/08/93	20:03:32	42	1.17	0.68	1.88
82	31/08/93	20:05:30	29	1.10	0.66	1.73
83	05/09/93	21:47:22	38	1.12	0.76	1.86
84	07/09/93	21:57:46	28	1.19	0.73	1.73
85	16/09/93	20:23:34	28	1.12	0.81	1.83
86	06/10/93	19:00:53	61	1.29	0.73	1.95
87	06/10/93	19:02:19	33	1.29	0.73	1.81
88	21/10/93	23:50:24	45	1.22	0.81	2.05
89	29/10/93	19:07:55	29	1.27	0.76	1.73
90	15/11/93	10:27:16	28	44.07 $^-$	9.89 $^-$	24.93 $^-$
91	15/11/93	10:29:12	28	34.86 $^-$	8.91 $^-$	15.19 $^-$
92	15/11/93	11:09:51	28	28.30 $^-$	7.81 $^-$	21.39 $^-$
93	17/11/93	09:49:06	28	49.98 $^-$	14.62 $^-$	34.26 $^-$
94	17/11/93	13:42:35	28	43.24 $^-$	50.00 $^-$	45.31 $^-$
95	18/11/93	21:56:28	28	3.27	0.78	1.93
96	25/11/93	23:59:10	33	3.22	0.78	2.00
97	07/12/93	09:12:44	28	37.60 $^-$	9.94 $^-$	33.76 $^-$
98	23/06/94	07:21:23	33	3.24	1.05	1.44
99	23/06/94	07:35:39	32	3.27	1.03	1.46
100	24/06/94	02:26:08	28	3.27	0.98	1.44
101	24/06/94	02:37:58	31	3.29	1.00	1.49
102	24/06/94	02:41:30	31	3.32	0.98	1.59
103	24/06/94	02:42:43	36	3.29	0.98	1.49
104	24/06/94	02:50:47	38	3.15	1.00	1.42
105	24/06/94	02:52:05	31	3.29	1.03	1.51

Table 2: *Date, time, duration and numerical maximal acceleration in the three directions.*

No.	Date	Time	Duration	A1 (%g)	A2 (%g)	A3 (%g)
			[sec]	$[m/s^2]$	$[m/s^2]$	$[m/s^2]$
106	24/06/94	03:17:31	42	3.24	0.98	1.56
107	24/06/94	03:46:35	20	3.37	1.00	1.44
108	24/06/94	20:24:17	28	3.25	0.98	1.44
109	25/06/94	10:17:49	28	3.25	1.10	1.39
110	25/06/94	10:18:27	28	3.25	1.05	1.42
111	25/06/94	22:01:36	28	3.25	1.00	1.42
112	26/06/94	09:51:39	28	3.22	1.03	1.39
113	26/06/94	09:55:02	31	3.25	1.05	1.42
114	26/06/94	09:56:27	38	3.25	1.07	1.39
115	26/06/94	10:12:46	33	3.27	1.07	1.46
116	26/06/94	10:37:17	44	3.32	1.07	1.54
117	27/06/94	05:20:34	28	3.20	1.07	1.42
118	27/06/94	05:48:38	36	3.17	1.05	1.46
119	28/06/94	09:08:27	28	3.17	1.07	1.46
120	29/06/94	09:15:44	28	11.87 –	8.89 –	12.35 –
121	29/06/94	09:20:59	28	30.96 –	50.00 –	28.05 –
122	30/06/94	21:53:21	28	3.49	1.17	1.46
123	30/06/94	22:04:15	31	3.25	1.15	1.54
124	01/07/94	07:51:37	28	3.15	1.03	1.46
125	01/07/94	11:20:35	28	3.15	1.12	1.44
126	01/07/94	19:10:24	33	3.13	1.12	1.61
127	01/07/94	19:15:33	28	3.17	1.03	1.51
128	01/07/94	19:17:25	42	3.15	1.05	1.61
129	01/07/94	19:20:30	33	3.08	1.05	1.59
130	02/07/94	07:17:53	28	3.15	1.00	1.49
131	02/07/94	07:23:17	28	3.13	1.00	1.49
132	02/07/94	07:38:22	36	3.22	1.00	1.61
133	03/07/94	14:25:11	44	3.15	1.03	1.78
134	03/07/94	15:36:03	28	3.10	1.03	1.49
135	03/07/94	20:07:15	28	3.15	0.95	1.44
136	04/07/94	21:16:57	28	3.34	1.00	1.49
137	04/07/94	23:26:04	28	3.15	1.00	1.46
138	05/07/94	17:11:20	28	3.17	1.03	1.49
139	05/07/94	17:19:02	40	3.15	1.05	1.59
140	05/07/94	17:20:11	47	3.27	1.05	1.68
141	05/07/94	17:21:14	38	3.20	1.07	1.64
142	05/07/94	17:28:22	31	3.13	1.05	1.49
143	07/07/94	08:15:33	28	3.30	1.15	1.42
144	08/07/94	10:57:51	33	3.17	1.00	1.59
145	11/07/94	10:01:18	33	3.15	1.05	1.54
146	13/07/94	09:39:26	38	3.22	1.05	1.76
147	13/07/94	10:09:03	38	19.12 –	42.87 –	1.95 –
148	14/07/94	17:57:00	55	3.13	1.03	1.64
149	15/07/94	06:55:48	48	3.25	1.05	1.68
150	15/07/94	07:14:42	31	3.15	1.03	1.49
151	15/07/94	13:21:00	28	3.15	1.07	1.42
152	17/07/94	19:27:42	50	3.17	1.03	1.68
153	17/07/94	19:28:26	38	3.15	1.03	1.66
154	17/07/94	19:35:15	31	3.15	1.00	1.51
155	18/07/94	14:42:47	41	3.10	1.07	1.64
156	19/07/94	05:26:33	56	3.20	1.05	1.56
157	19/07/94	05:35:57	49	3.30	1.05	1.83
158	19/07/94	05:41:12	47	3.20	1.05	1.59
159	19/07/94	05:43:08	28	3.20	1.07	1.46
160	20/07/94	08:03:46	45	3.15	1.05	1.59

Table 3: *Date, time, duration and numerical maximal acceleration in the three directions*

No.	Direction	Mean	Std. dev.	Skewness	Kurtosis
1	A1	5.314e-3	1.658e-2	-1.517e-1	1.731e+0
	A2	-2.022e-2	4.004e-3	3.849e-3	2.137e+0
	A3	-1.309e-2	5.035e-2	-4.443e+0	1.641e+0
2	A1	2.549e-3	8.630e-3	-3.485e-3	2.562e+0
	A2	-2.228e-2	4.912e-3	2.287e-3	2.029e+0
	A3	-1.333e-2	2.365e-2	-6.571e-1	1.914e+0
3	A1	2.644e-3	9.190e-3	-5.384e-2	2.239e+0
	A2	-2.227e-2	4.906e-3	2.585e-3	1.996e+0
	A3	-1.366e-2	2.564e-2	-1.360e-1	1.717e+0
4	A1	2.820e-3	8.852e-3	-1.088e-1	2.068e+0
	A2	-2.232e-2	4.889e-3	3.599e-3	2.021e+0
	A3	-1.407e-2	2.467e-2	1.398e-1	1.748e+0
5	A1	2.131e-3	8.298e-3	-4.689e-2	2.319e+0
	A2	-2.233e-2	4.929e-3	-8.138e-3	2.102e+0
	A3	-1.321e-2	2.257e-2	-1.278e-1	1.741e+0
6	A1	6.296e-3	8.616e-3	-3.679e-2	2.180e+0
	A2	-2.253e-2	4.823e-3	6.680e-3	1.752e+0
	A3	-1.434e-2	2.551e-2	-7.359e-1	1.693e+0
7	A1	6.365e-3	8.295e-3	5.989e-3	2.446e+0
	A2	-2.254e-2	5.082e-3	7.927e-3	1.705e+0
	A3	-1.458e-2	2.320e-2	-8.103e-2	1.990e+0
8	A1	6.378e-3	8.021e-3	-7.975e-2	2.224e+0
	A2	-2.254e-2	4.807e-3	6.703e-3	1.725e+0
	A3	-1.495e-2	2.383e-2	1.318e-1	1.728e+0
9	A1	6.042e-3	9.294e-3	-1.076e-1	2.207e+0
	A2	-2.246e-2	3.961e-3	1.850e-3	1.900e+0
	A3	-1.451e-2	2.690e-2	-1.462e-1	1.995e+0
10	A1	5.839e-3	9.898e-3	-1.322e-2	2.200e+0
	A2	-2.228e-2	5.345e-3	-1.453e-2	1.986e+0
	A3	-1.354e-2	3.241e-2	8.436e-2	1.926e+0
11	A1	6.398e-3	9.268e-3	-3.512e-2	2.112e+0
	A2	-2.332e-2	4.561e-3	-2.039e-3	1.971e+0
	A3	-1.535e-2	2.593e-2	-3.514e-1	1.769e+0
12	A1	5.761e-3	1.081e-2	-6.576e-2	2.053e+0
	A2	-2.277e-2	3.641e-3	-4.320e-3	2.159e+0
	A3	-1.440e-2	3.461e-2	-1.289e-1	1.867e+0
13	A1	1.984e-2	9.696e-3	-3.727e-2	2.074e+0
	A2	-2.573e-2	3.525e-3	2.761e-3	2.632e+0
	A3	-1.010e-2	3.085e-2	-7.212e-1	1.852e+0
14	A1	1.981e-2	8.165e-3	8.317e-3	1.913e+0
	A2	-2.489e-2	2.981e-3	-4.710e-4	2.478e+0
	A3	-9.043e-3	2.618e-2	-1.719e-1	1.589e+0
15	A1	2.014e-2	8.708e-3	1.808e-3	1.875e+0
	A2	-2.368e-2	2.875e-3	-3.411e-3	2.715e+0
	A3	-7.956e-3	2.608e-2	-1.054e-2	1.620e+0
16	A1	2.000e-2	9.527e-3	-5.610e-2	1.979e+0
	A2	-2.376e-2	3.111e-3	-5.231e-3	2.639e+0
	A3	-7.585e-3	2.909e-2	-8.860e-1	1.759e+0
17	A1	2.003e-2	7.865e-3	-4.119e-3	1.916e+0
	A2	-2.376e-2	3.222e-3	-5.179e-3	2.583e+0
	A3	-7.602e-3	2.440e-2	-5.388e-1	1.645e+0
18	A1	1.999e-2	8.475e-3	-2.830e-2	1.862e+0
	A2	-2.385e-2	3.123e-3	-5.281e-3	2.639e+0
	A3	-7.447e-3	2.522e-2	-6.560e-1	1.587e+0

Table 4: *Mean, standard deviation, skewness and kurtosis of the measurements in each directions.*

No.	Direction	Mean	Std. dev.	Skewness	Kurtosis
19	A1	2.007e-2	8.476e-3	-4.501e-2	2.526e+0
	A2	-2.393e-2	3.153e-3	-5.080e-3	2.528e+0
	A3	-8.039e-3	2.676e-2	-2.664e-1	2.171e+0
20	A1	1.997e-2	8.403e-3	-3.202e-2	2.190e+0
	A2	-2.396e-2	3.066e-3	-5.050e-3	2.585e+0
	A3	-7.909e-3	2.557e-2	-2.881e-1	1.748e+0
21	A1	2.026e-2	8.164e-3	-7.762e-2	1.919e+0
	A2	-2.402e-2	2.896e-3	-3.764e-3	2.671e+0
	A3	-8.604e-3	2.561e-2	4.103e-1	1.676e+0
22	A1	1.995e-2	9.259e-3	-3.224e-2	1.897e+0
	A2	-2.428e-2	3.163e-3	-6.568e-3	2.602e+0
	A3	-8.205e-3	2.675e-2	-7.002e-1	1.656e+0
23	A1	1.937e-2	9.780e-3	-7.154e-2	2.294e+0
	A2	-2.592e-2	3.477e-3	-3.259e-3	2.346e+0
	A3	-9.967e-3	2.896e-2	-2.690e-1	1.942e+0
24	A1	1.927e-2	9.607e-3	-1.387e-1	2.267e+0
	A2	-2.581e-2	3.657e-3	-4.864e-3	2.269e+0
	A3	-9.667e-3	2.986e-2	-9.072e-1	2.033e+0
25	A1	2.082e-2	1.002e-2	-4.446e-2	2.061e+0
	A2	-2.306e-2	2.551e-3	2.309e-3	2.854e+0
	A3	-6.943e-3	3.039e-2	-2.129e-1	1.736e+0
26	A1	2.089e-2	8.456e-3	-5.483e-2	2.239e+0
	A2	-2.311e-2	2.593e-3	2.235e-3	2.799e+0
	A3	-7.181e-3	2.430e-2	1.938e-1	1.944e+0
27	A1	2.094e-2	9.250e-3	-5.655e-2	2.253e+0
	A2	-2.316e-2	2.700e-3	2.567e-3	2.721e+0
	A3	-7.400e-3	2.687e-2	2.877e-1	1.782e+0
28	A1	2.089e-2	8.626e-3	-3.648e-2	2.010e+0
	A2	-2.318e-2	2.649e-3	1.713e-3	2.778e+0
	A3	-7.304e-3	2.383e-2	2.139e-1	2.072e+0
29	A1	2.078e-2	8.747e-3	-1.852e-2	2.256e+0
	A2	-2.318e-2	2.586e-3	2.458e-3	2.824e+0
	A3	-7.110e-3	2.613e-2	-1.394e-1	1.688e+0
30	A1	2.058e-2	7.876e-3	1.309e-2	2.621e+0
	A2	-2.327e-2	2.814e-3	1.773e-3	2.599e+0
	A3	-6.946e-3	2.194e-2	-4.571e-1	2.107e+0
31	A1	2.095e-2	8.267e-3	-5.155e-2	2.118e+0
	A2	-2.329e-2	2.822e-3	2.295e-3	2.682e+0
	A3	-7.604e-3	2.555e-2	4.526e-1	1.925e+0
32	A1	2.092e-2	7.341e-3	-1.630e-2	2.569e+0
	A2	-2.335e-2	2.849e-3	1.997e-3	2.462e+0
	A3	-7.728e-3	2.138e-2	2.166e-1	2.122e+0
33	A1	1.956e-2	9.197e-3	3.029e-2	2.217e+0
	A2	-2.617e-2	1.982e-3	-7.779e-4	2.876e+0
	A3	-1.005e-2	2.624e-2	-1.681e-1	1.722e+0
34	A1	2.055e-2	8.772e-3	2.364e-2	2.865e+0
	A2	-2.368e-2	2.856e-3	-1.312e-3	2.643e+0
	A3	-7.426e-3	2.267e-2	-1.204e-1	1.859e+0
35	A1	2.065e-2	9.785e-3	-3.954e-2	2.414e+0
	A2	-2.370e-2	2.665e-3	-1.350e-3	2.759e+0
	A3	-7.349e-3	2.465e-2	-2.158e-1	1.792e+0
36	A1	2.147e-2	9.079e-3	-1.617e-2	2.000e+0
	A2	-2.252e-2	4.837e-3	5.530e-3	1.905e+0
	A3	-5.284e-3	2.607e-2	-1.733e-1	1.603e+0

Table 5: *Mean, standard deviation, skewness and kurtosis of the measurements in each directions.*

No.	Direction	Mean	Std. dev.	Skewness	Kurtosis
37	A1	2.009e-2	1.078e-2	-6.152e-2	2.140e+0
	A2	-2.571e-2	4.887e-3	2.050e-2	2.209e+0
	A3	-8.914e-3	3.393e-2	-2.446e-1	2.075e+0
38	A1	2.036e-2	8.241e-3	-5.500e-2	1.925e+0
	A2	-2.554e-2	3.940e-3	-2.596e-3	1.928e+0
	A3	-8.390e-3	2.548e-2	-8.935e-2	1.617e+0
39	A1	2.039e-2	8.337e-3	-6.170e-2	2.058e+0
	A2	-2.499e-2	5.920e-3	-8.274e-2	2.161e+0
	A3	-8.271e-3	2.437e-2	7.495e-1	1.668e+0
40	A1	2.239e-2	7.658e-3	-3.521e-2	2.271e+0
	A2	-2.087e-2	2.212e-3	-4.825e-4	2.648e+0
	A3	-2.869e-3	2.392e-2	7.311e-2	2.272e+0
41	A1	2.027e-2	8.343e-3	-7.352e-2	2.577e+0
	A2	-2.594e-2	3.592e-3	-3.746e-3	2.411e+0
	A3	-8.714e-3	2.406e-2	-2.593e-1	1.795e+0
42	A1	2.031e-2	7.713e-3	5.683e-3	2.382e+0
	A2	-2.591e-2	3.502e-3	-2.829e-3	2.384e+0
	A3	-8.945e-3	2.287e-2	1.373e-1	2.475e+0
43	A1	2.030e-2	7.832e-3	-6.060e-2	2.409e+0
	A2	-2.589e-2	3.810e-3	-5.184e-3	2.318e+0
	A3	-8.985e-3	2.162e-2	1.002e-1	2.149e+0
44	A1	1.991e-2	7.400e-3	-1.080e-2	2.388e+0
	A2	-2.683e-2	2.445e-3	2.251e-3	2.627e+0
	A3	-9.486e-3	2.264e-2	-4.217e-1	1.902e+0
45	A1	1.992e-2	7.984e-3	-1.821e-2	2.117e+0
	A2	-2.683e-2	2.588e-3	2.092e-3	2.553e+0
	A3	-9.248e-3	2.393e-2	-7.093e-1	1.777e+0
46	A1	2.088e-2	7.762e-3	-2.388e-2	2.327e+0
	A2	-2.402e-2	3.222e-3	1.791e-3	2.061e+0
	A3	-6.324e-3	2.281e-2	-6.490e-1	2.017e+0
47	A1	2.032e-2	8.246e-3	-2.013e-2	1.982e+0
	A2	-2.594e-2	4.154e-3	2.143e-3	2.210e+0
	A3	-8.624e-3	2.402e-2	-5.139e-1	1.641e+0
48	A1	2.065e-2	8.684e-3	-5.509e-2	2.264e+0
	A2	-2.583e-2	3.847e-3	-9.651e-3	2.053e+0
	A3	-8.965e-3	2.366e-2	2.123e-1	1.764e+0
49	A1	2.033e-2	8.715e-3	-2.599e-2	2.177e+0
	A2	-2.573e-2	4.235e-3	-1.345e-2	1.936e+0
	A3	-8.157e-3	2.453e-2	-9.564e-1	1.781e+0
50	A1	2.052e-2	8.538e-3	-2.678e-2	1.840e+0
	A2	-2.613e-2	2.854e-3	-1.362e-3	2.185e+0
	A3	-8.920e-3	2.913e-2	-1.513e-1	1.748e+0
51	A1	2.060e-2	8.644e-3	-7.064e-2	2.182e+0
	A2	-2.607e-2	2.674e-3	-6.385e-4	2.176e+0
	A3	-9.445e-3	2.527e-2	3.133e-1	1.772e+0
52	A1	2.046e-2	9.462e-3	-2.284e-2	2.194e+0
	A2	-2.607e-2	2.872e-3	-9.829e-4	2.605e+0
	A3	-8.907e-3	2.774e-2	-9.945e-2	1.765e+0
53	A1	2.054e-2	7.496e-3	1.565e-2	2.247e+0
	A2	-2.625e-2	3.484e-3	-1.934e-3	1.956e+0
	A3	-9.266e-3	2.364e-2	-1.086e-1	1.821e+0
54	A1	2.037e-2	8.246e-3	2.637e-2	2.078e+0
	A2	-2.625e-2	3.563e-3	-1.812e-3	1.945e+0
	A3	-8.607e-3	2.400e-2	-2.913e-1	1.821e+0

Table 6: *Mean, standard deviation, skewness and kurtosis of the measurements in each directions.*

No.	Direction	Mean	Std. dev.	Skewness	Kurtosis
55	A1	2.003e-2	7.178e-3	-1.119e-2	2.110e+0
	A2	-2.622e-2	3.320e-3	-3.736e-3	2.503e+0
	A3	-8.761e-3	2.364e-2	-1.331e-1	1.634e+0
56	A1	2.182e-2	9.311e-3	-7.791e-2	2.121e+0
	A2	-2.230e-2	3.449e-3	-1.056e-3	2.220e+0
	A3	-3.851e-3	2.421e-2	-9.072e-2	1.928e+0
57	A1	2.189e-2	9.786e-3	4.770e-3	2.489e+0
	A2	-2.259e-2	3.232e-3	-4.598e-4	2.244e+0
	A3	-4.650e-3	2.457e-2	4.482e-1	1.665e+0
58	A1	2.126e-2	9.205e-3	-5.002e-2	1.861e+0
	A2	-2.515e-2	3.354e-3	-1.465e-3	2.168e+0
	A3	-7.350e-3	2.770e-2	-5.696e-2	1.597e+0
59	A1	2.115e-2	8.919e-3	-3.773e-2	2.064e+0
	A2	-2.515e-2	3.151e-3	-1.227e-3	2.125e+0
	A3	-6.897e-3	2.758e-2	-7.123e-1	1.655e+0
60	A1	2.123e-2	8.824e-3	-3.815e-2	1.903e+0
	A2	-2.516e-2	3.153e-3	-1.235e-3	2.113e+0
	A3	-7.258e-3	2.706e-2	-1.038e-1	1.788e+0
61	A1	2.136e-2	1.012e-2	-9.135e-2	2.270e+0
	A2	-2.518e-2	3.457e-3	-2.775e-3	2.068e+0
	A3	-7.603e-3	2.917e-2	3.270e-1	1.737e+0
62	A1	2.116e-2	8.337e-3	5.357e-4	1.830e+0
	A2	-2.520e-2	3.489e-3	-2.290e-3	1.997e+0
	A3	-7.060e-3	2.483e-2	-2.560e-1	1.614e+0
63	A1	2.129e-2	9.268e-3	-2.241e-2	1.828e+0
	A2	-2.521e-2	3.579e-3	-3.848e-3	2.044e+0
	A3	-7.436e-3	2.787e-2	-1.961e-1	1.597e+0
64	A1	2.121e-2	9.296e-3	-3.005e-2	2.029e+0
	A2	-2.523e-2	3.893e-3	-5.158e-3	2.005e+0
	A3	-7.263e-3	2.960e-2	-3.490e-1	1.667e+0
65	A1	2.112e-2	9.033e-3	-2.794e-2	2.051e+0
	A2	-2.522e-2	3.952e-3	-4.485e-3	1.965e+0
	A3	-7.099e-3	2.740e-2	-4.766e-1	1.680e+0
66	A1	2.131e-2	8.672e-3	-4.974e-2	1.861e+0
	A2	-2.525e-2	4.103e-3	-4.772e-3	1.931e+0
	A3	-7.444e-3	2.566e-2	-5.591e-2	1.625e+0
67	A1	2.131e-2	8.878e-3	-6.526e-2	2.016e+0
	A2	-2.527e-2	4.073e-3	-5.063e-3	1.932e+0
	A3	-7.505e-3	2.742e-2	1.440e-1	1.783e+0
68	A1	2.118e-2	7.430e-3	-6.708e-3	2.224e+0
	A2	-2.546e-2	3.674e-3	-1.202e-3	1.985e+0
	A3	-7.309e-3	2.290e-2	-3.695e-1	1.885e+0
69	A1	2.111e-2	8.704e-3	1.030e-2	2.005e+0
	A2	-2.569e-2	4.234e-3	-1.997e-3	1.826e+0
	A3	-7.584e-3	2.513e-2	-5.751e-1	1.652e+0
70	A1	2.111e-2	8.091e-3	1.185e-2	1.909e+0
	A2	-2.568e-2	4.165e-3	-3.153e-3	1.838e+0
	A3	-7.679e-3	2.460e-2	-2.919e-1	1.623e+0
71	A1	2.116e-2	6.842e-3	2.119e-2	2.131e+0
	A2	-2.594e-2	4.697e-3	-5.042e-3	1.759e+0
	A3	-8.074e-3	1.910e-2	-2.246e-1	2.435e+0
72	A1	2.111e-2	7.844e-3	-2.500e-2	1.969e+0
	A2	-2.187e-2	4.677e-3	4.793e-3	2.263e+0
	A3	-2.695e-3	2.351e-2	-2.956e-1	1.785e+0

Table 7: *Mean, standard deviation, skewness and kurtosis of the measurements in each directions.*

No.	Direction	Mean	Std. dev.	Skewness	Kurtosis
73	A1	2.231e-2	9.577e-3	-2.355e-2	2.070e+0
	A2	-2.503e-2	3.210e-3	3.855e-4	2.961e+0
	A3	-6.177e-3	2.922e-2	-7.627e-1	1.663e+0
74	A1	2.238e-2	8.272e-3	-1.841e-2	2.091e+0
	A2	-2.446e-2	5.145e-3	-1.092e-2	2.039e+0
	A3	-5.600e-3	2.572e-2	6.929e-1	1.827e+0
75	A1	2.229e-2	8.981e-3	-5.974e-2	2.410e+0
	A2	-2.504e-2	4.433e-3	-3.701e-3	2.125e+0
	A3	-6.539e-3	2.515e-2	1.186e-1	1.639e+0
76	A1	2.210e-2	8.351e-3	-7.638e-2	1.933e+0
	A2	-2.513e-2	4.455e-3	-5.236e-3	2.142e+0
	A3	-6.110e-3	2.579e-2	-5.178e-1	1.625e+0
77	A1	2.212e-2	9.951e-3	-4.440e-2	2.216e+0
	A2	-2.531e-2	4.655e-3	-4.249e-3	2.138e+0
	A3	-6.483e-3	2.957e-2	-2.970e-1	2.118e+0
78	A1	2.211e-2	8.826e-3	-4.153e-2	1.987e+0
	A2	-2.542e-2	4.696e-3	-2.675e-3	2.101e+0
	A3	-6.900e-3	2.602e-2	-2.189e-1	1.562e+0
79	A1	2.209e-2	8.493e-3	-2.014e-2	2.014e+0
	A2	-2.546e-2	4.907e-3	-3.312e-4	2.129e+0
	A3	-6.813e-3	2.516e-2	-1.413e-1	1.599e+0
80	A1	2.350e-2	1.595e-2	-2.871e-1	1.724e+0
	A2	-2.446e-2	2.512e-3	3.065e-4	2.809e+0
	A3	-3.767e-3	4.859e-2	1.551e+0	1.607e+0
81	A1	2.362e-2	1.628e-2	-3.667e-2	1.938e+0
	A2	-2.609e-2	2.280e-3	-6.160e-5	2.642e+0
	A3	-5.549e-3	4.893e-2	-1.211e+0	1.774e+0
82	A1	2.333e-2	1.497e-2	-1.348e-1	1.781e+0
	A2	-2.614e-2	2.252e-3	3.061e-4	2.667e+0
	A3	-4.768e-3	4.671e-2	-3.747e+0	1.657e+0
83	A1	2.325e-2	1.557e-2	-9.782e-2	1.788e+0
	A2	-2.888e-2	2.607e-3	-3.906e-4	2.859e+0
	A3	-8.174e-3	4.932e-2	-8.394e-1	1.650e+0
84	A1	2.331e-2	1.571e-2	-5.948e-2	1.777e+0
	A2	-2.843e-2	2.794e-3	6.066e-4	2.655e+0
	A3	-7.940e-3	4.645e-2	-5.821e-1	1.578e+0
85	A1	2.392e-2	1.480e-2	-1.067e-1	1.897e+0
	A2	-2.813e-2	3.757e-3	-2.263e-3	2.387e+0
	A3	-6.858e-3	4.581e-2	-2.251e+0	1.640e+0
86	A1	2.619e-2	1.740e-2	1.915e-1	1.894e+0
	A2	-2.653e-2	3.162e-3	2.341e-3	2.817e+0
	A3	-4.654e-3	5.332e-2	-6.274e-2	1.725e+0
87	A1	2.609e-2	1.543e-2	1.053e-1	2.072e+0
	A2	-2.654e-2	3.143e-3	1.870e-3	2.779e+0
	A3	-4.503e-3	4.865e-2	1.037e+0	1.655e+0
88	A1	2.618e-2	1.684e-2	-1.331e-2	1.866e+0
	A2	-2.981e-2	3.624e-3	1.506e-3	2.468e+0
	A3	-7.065e-3	5.131e-2	-1.028e+0	1.728e+0
89	A1	2.773e-2	1.615e-2	1.641e-1	1.883e+0
	A2	-2.725e-2	3.313e-3	-4.605e-3	2.444e+0
	A3	-3.842e-3	4.674e-2	-2.829e+0	1.655e+0
90	A1	2.625e-2	8.703e-2	3.580e+3	1.885e+2
	A2	-3.242e-2	2.271e-2	1.018e+2	2.225e+2
	A3	-8.242e-3	3.432e-2	-6.576e+2	6.087e+2

Table 8: *Mean, standard deviation, skewness and kurtosis of the measurements in each directions.*

No.	Direction	Mean	Std. dev.	Skewness	Kurtosis
91	A1	2.584e-2	6.138e-2	3.074e+3	3.467e+2
	A2	-3.247e-2	1.690e-2	7.333e+1	3.914e+2
	A3	-8.716e-3	2.147e-2	-1.234e+2	4.050e+2
92	A1	2.636e-2	5.972e-2	1.195e+3	2.851e+2
	A2	-3.214e-2	1.674e-2	3.622e+1	3.112e+2
	A3	-8.297e-3	2.582e-2	-2.261e+2	6.033e+2
93	A1	2.315e-2	1.281e-1	1.215e+4	1.136e+2
	A2	-3.089e-2	3.389e-2	3.756e+2	1.796e+2
	A3	-6.495e-3	5.516e-2	-2.378e+3	4.082e+2
94	A1	1.010e-1	1.721e-1	1.136e+4	5.756e+1
	A2	-2.765e-2	1.110e-1	-6.438e+3	2.490e+2
	A3	1.089e-2	9.223e-2	1.312e+1	2.651e+2
95	A1	1.285e-1	1.585e-2	2.661e-1	1.882e+0
	A2	-3.039e-2	2.906e-3	4.338e-4	2.442e+0
	A3	1.649e-2	4.486e-2	-1.940e+0	1.687e+0
96	A1	1.266e-1	1.719e-2	2.633e-1	1.750e+0
	A2	-3.106e-2	2.606e-3	1.702e-3	2.459e+0
	A3	1.457e-2	4.655e-2	1.356e+0	1.705e+0
97	A1	1.246e-1	8.747e-2	3.569e+3	1.703e+2
	A2	-3.444e-2	2.508e-2	1.005e+2	1.806e+2
	A3	1.085e-2	3.932e-2	-1.106e+3	7.577e+2
98	A1	1.363e-1	1.211e-2	8.075e-3	1.844e+0
	A2	-4.091e-2	3.424e-3	5.701e-3	2.353e+0
	A3	1.275e-2	3.369e-2	3.562e-1	1.589e+0
99	A1	1.366e-1	1.198e-2	1.516e-3	2.123e+0
	A2	-4.098e-2	3.763e-3	3.931e-3	2.496e+0
	A3	1.216e-2	3.340e-2	1.616e+0	1.633e+0
100	A1	1.354e-1	1.130e-2	7.818e-2	2.140e+0
	A2	-3.794e-2	4.215e-3	3.961e-3	2.277e+0
	A3	1.629e-2	2.913e-2	-4.933e-1	1.801e+0
101	A1	1.357e-1	1.073e-2	-6.144e-2	2.217e+0
	A2	-3.794e-2	4.070e-3	2.930e-3	2.274e+0
	A3	1.586e-2	3.142e-2	-4.404e-1	1.717e+0
102	A1	1.356e-1	1.246e-2	-3.967e-2	2.393e+0
	A2	-3.793e-2	3.906e-3	4.262e-3	2.203e+0
	A3	1.616e-2	2.905e-2	-1.760e-1	1.999e+0
103	A1	1.356e-1	1.209e-2	2.861e-2	2.161e+0
	A2	-3.793e-2	4.061e-3	1.280e-3	2.168e+0
	A3	1.583e-2	3.294e-2	7.184e-1	1.672e+0
104	A1	1.355e-1	9.979e-3	7.476e-2	1.929e+0
	A2	-3.792e-2	3.997e-3	2.061e-4	2.154e+0
	A3	1.651e-2	3.056e-2	-1.027e+0	1.631e+0
105	A1	1.355e-1	1.182e-2	1.107e-1	2.257e+0
	A2	-3.791e-2	4.102e-3	5.174e-4	2.246e+0
	A3	1.611e-2	3.202e-2	3.451e-1	1.725e+0
106	A1	1.357e-1	1.156e-2	5.393e-2	1.954e+0
	A2	-3.787e-2	4.043e-3	1.555e-3	2.321e+0
	A3	1.597e-2	3.301e-2	3.884e-1	1.724e+0
107	A1	1.356e-1	1.264e-2	-4.573e-2	2.509e+0
	A2	-3.793e-2	4.032e-3	5.690e-5	2.360e+0
	A3	1.619e-2	3.211e-2	-6.883e-1	1.606e+0
108	A1	1.359e-1	1.030e-2	1.554e-1	2.273e+0
	A2	3.773e-2	3.691e-3	-7.283e-3	2.296e+0
	A3	1.658e-2	2.965e-2	3.821e-1	1.794e+0

Table 9: *Mean, standard deviation, skewness and kurtosis of the measurements in each directions.*

No.	Direction	Mean	Std. dev.	Skewness	Kurtosis
109	A1	1.355e-1	1.137e-2	4.822e-2	2.039e+0
	A2	-4.064e-2	4.570e-3	-2.233e-2	2.036e+0
	A3	1.379e-2	3.240e-2	-1.045e+0	1.583e+0
110	A1	1.355e-1	1.143e-2	1.036e-1	2.218e+0
	A2	-4.063e-2	4.519e-3	-2.551e-2	1.946e+0
	A3	1.358e-2	2.898e-2	3.031e-1	1.838e+0
111	A1	1.358e-1	1.055e-2	5.086e-2	1.990e+0
	A2	-3.961e-2	4.109e-3	-5.329e-3	2.188e+0
	A3	1.459e-2	3.133e-2	-6.990e-1	1.592e+0
112	A1	1.357e-1	1.038e-2	-3.009e-2	2.061e+0
	A2	-4.160e-2	3.752e-3	4.936e-3	2.234e+0
	A3	1.241e-2	2.923e-2	-3.831e-1	1.721e+0
113	A1	1.358e-1	1.141e-2	-3.721e-2	2.115e+0
	A2	-4.159e-2	3.812e-3	2.517e-3	2.305e+0
	A3	1.202e-2	3.042e-2	3.833e-1	1.687e+0
114	A1	1.357e-1	1.060e-2	-3.309e-2	2.114e+0
	A2	-4.159e-2	4.027e-3	7.185e-3	2.402e+0
	A3	1.258e-2	3.036e-2	-9.643e-1	1.672e+0
115	A1	1.359e-1	1.027e-2	6.961e-2	2.194e+0
	A2	-4.158e-2	4.269e-3	-2.328e-3	2.261e+0
	A3	1.196e-2	3.141e-2	3.122e-1	1.749e+0
116	A1	1.358e-1	1.164e-2	-2.047e-2	2.165e+0
	A2	-4.158e-2	4.202e-3	-1.024e-2	2.119e+0
	A3	1.207e-2	3.411e-2	5.749e-1	1.772e+0
117	A1	1.360e-1	1.095e-2	-7.755e-2	2.146e+0
	A2	-4.107e-2	4.291e-3	2.187e-3	2.275e+0
	A3	1.220e-2	2.974e-2	1.347e+0	1.753e+0
118	A1	1.358e-1	1.072e-2	1.449e-2	1.844e+0
	A2	-4.105e-2	4.122e-3	1.194e-4	2.090e+0
	A3	1.264e-2	3.225e-2	6.273e-1	1.753e+0
119	A1	1.356e-1	1.026e-2	5.178e-2	2.102e+0
	A2	-3.978e-2	5.172e-3	-1.521e-2	1.952e+0
	A3	1.427e-2	2.917e-2	-6.747e-1	1.784e+0
120	A1	1.357e-1	1.382e-2	4.056e+0	5.198e+2
	A2	-4.141e-2	9.933e-3	1.276e+1	1.292e+3
	A3	1.245e-2	1.853e-2	-1.796e+1	3.591e+2
121	A1	1.351e-1	5.025e-2	-1.316e+3	5.564e+2
	A2	-4.172e-2	1.051e-1	4.677e+3	5.139e+2
	A3	1.487e-2	4.847e-2	2.810e+1	5.600e+2
122	A1	1.347e-1	1.116e-2	-9.429e-3	2.532e+0
	A2	-3.959e-2	4.791e-3	-6.420e-3	2.598e+0
	A3	1.787e-2	2.703e-2	6.042e-1	1.754e+0
123	A1	1.345e-1	1.145e-2	4.780e-2	2.172e+0
	A2	-3.974e-2	2.992e-3	-3.559e-3	4.055e+0
	A3	1.842e-2	3.237e-2	-4.746e-1	1.613e+0
124	A1	1.340e-1	9.250e-3	1.033e-1	2.104e+0
	A2	-4.144e-2	4.152e-3	1.567e-2	1.949e+0
	A3	1.674e-2	2.976e-2	7.958e-2	1.691e+0
125	A1	1.336e-1	9.324e-3	1.030e-3	2.281e+0
	A2	-4.158e-2	5.153e-3	-1.435e-3	2.057e+0
	A3	1.707e-2	2.817e-2	-3.305e-1	1.762e+0
126	A1	1.334e-1	1.002e-2	5.416e-2	1.910e+0
	A2	-4.028e-2	4.743e-3	-4.384e-3	2.109e+0
	A3	1.810e-2	3.080e-2	4.235e-1	1.823e+0

Table 10: *Mean, standard deviation, skewness and kurtosis of the measurements in each directions.*

No.	Direction	Mean	Std. dev.	Skewness	Kurtosis
127	A1	1.335e-1	9.613e-3	7.059e-2	2.132e+0
	A2	-4.033e-2	4.715e-3	-3.402e-3	1.908e+0
	A3	1.843e-2	3.002e-2	-8.110e-2	1.658e+0
128	A1	1.334e-1	1.045e-2	2.144e-2	1.992e+0
	A2	-4.033e-2	4.697e-3	-4.163e-3	1.985e+0
	A3	1.866e-2	3.423e-2	-9.296e-1	1.662e+0
129	A1	1.335e-1	9.288e-3	2.429e-2	1.916e+0
	A2	-4.034e-2	4.880e-3	-1.425e-3	1.938e+0
	A3	1.830e-2	3.068e-2	1.005e-1	1.754e+0
130	A1	1.338e-1	9.446e-3	8.245e-2	2.462e+0
	A2	-4.064e-2	4.085e-3	1.294e-2	2.044e+0
	A3	1.783e-2	2.780e-2	-1.380e-2	1.885e+0
131	A1	1.338e-1	9.682e-3	1.128e-1	1.929e+0
	A2	-4.070e-2	4.025e-3	1.083e-2	1.958e+0
	A3	1.774e-2	3.106e-2	-4.222e-1	1.630e+0
132	A1	1.339e-1	1.096e-2	-3.649e-2	2.390e+0
	A2	-4.082e-2	4.209e-3	1.449e-2	2.137e+0
	A3	1.703e-2	3.279e-2	-8.934e-2	1.731e+0
133	A1	1.331e-1	9.922e-3	2.609e-2	2.106e+0
	A2	-4.049e-2	4.067e-3	-7.233e-3	2.084e+0
	A3	1.782e-2	3.414e-2	3.122e-1	2.058e+0
134	A1	1.337e-1	1.003e-2	3.137e-2	1.802e+0
	A2	-4.059e-2	4.356e-3	-9.199e-3	1.934e+0
	A3	1.823e-2	3.277e-2	-7.569e-1	1.586e+0
135	A1	1.338e-1	9.716e-3	-6.452e-3	2.194e+0
	A2	-4.052e-2	2.235e-3	4.321e-4	2.741e+0
	A3	1.803e-2	2.798e-2	-7.175e-1	1.789e+0
136	A1	1.334e-1	1.170e-2	3.805e-2	2.279e+0
	A2	-4.029e-2	3.455e-3	3.407e-3	2.366e+0
	A3	1.823e-2	3.284e-2	5.967e-1	1.582e+0
137	A1	1.337e-1	1.061e-2	8.745e-2	2.105e+0
	A2	-4.170e-2	3.212e-3	2.612e-5	2.272e+0
	A3	1.702e-2	2.987e-2	-5.289e-1	1.648e+0
138	A1	1.333e-1	1.094e-2	1.369e-1	1.935e+0
	A2	-4.147e-2	3.845e-3	-6.777e-3	1.985e+0
	A3	1.754e-2	3.291e-2	-2.205e-1	1.618e+0
139	A1	1.334e-1	1.080e-2	6.110e-2	1.926e+0
	A2	-4.144e-2	4.011e-3	-4.432e-3	2.013e+0
	A3	1.728e-2	3.260e-2	3.290e-2	1.832e+0
140	A1	1.333e-1	1.130e-2	2.055e-2	2.164e+0
	A2	-4.143e-2	4.139e-3	-3.688e-3	2.030e+0
	A3	1.702e-2	3.410e-2	2.365e-1	2.003e+0
141	A1	1.334e-1	1.139e-2	-3.531e-2	2.206e+0
	A2	-4.143e-2	4.226e-3	-4.489e-3	2.202e+0
	A3	1.707e-2	3.242e-2	5.999e-1	1.882e+0
142	A1	1.333e-1	1.057e-2	4.723e-2	1.885e+0
	A2	-4.143e-2	4.174e-3	-4.494e-3	1.928e+0
	A3	1.764e-2	3.187e-2	-6.952e-1	1.650e+0
143	A1	1.339e-1	1.098e-2	1.035e-1	2.064e+0
	A2	-4.347e-2	2.384e-3	4.180e-4	3.773e+0
	A3	1.478e-2	3.123e-2	2.094e-1	1.610e+0
144	A1	1.334e-1	9.841e-3	1.344e-2	2.040e+0
	A2	-4.132e-2	3.581e-3	-4.426e-3	2.053e+0
	A3	1.685e-2	3.095e-2	3.560e-1	1.786e+0

Table 11: *Mean, standard deviation, skewness and kurtosis of the measurements in each directions.*

No.	Direction	Mean	Std. dev.	Skewness	Kurtosis
145	A1	1.336e-1	1.090e-2	-3.412e-2	1.845e+0
	A2	-4.037e-2	5.104e-3	-1.904e-2	1.881e+0
	A3	1.763e-2	3.256e-2	-2.244e-1	1.674e+0
146	A1	1.337e-1	1.176e-2	-5.728e-2	2.020e+0
	A2	-4.141e-2	4.970e-3	-1.769e-2	1.877e+0
	A3	1.649e-2	3.663e-2	2.453e-1	1.736e+0
147	A1	1.332e-1	2.283e-2	1.054e+2	8.202e+2
	A2	-4.157e-2	5.634e-2	5.914e+2	8.953e+2
	A3	1.627e-2	2.579e-2	-3.911e+1	8.344e+2
148	A1	1.340e-1	1.043e-2	3.412e-2	1.881e+0
	A2	-4.022e-2	3.634e-3	-1.200e-2	2.192e+0
	A3	1.779e-2	3.493e-2	9.908e-2	1.741e+0
149	A1	1.335e-1	1.153e-2	-6.071e-3	2.072e+0
	A2	-4.299e-2	3.229e-3	-1.124e-3	2.308e+0
	A3	1.512e-2	3.602e-2	-4.515e-1	1.751e+0
150	A1	1.334e-1	1.086e-2	4.248e-2	1.851e+0
	A2	-4.299e-2	3.247e-3	-2.855e-3	2.218e+0
	A3	1.529e-2	3.264e-2	1.408e-1	1.596e+0
151	A1	1.330e-1	9.580e-3	9.600e-2	1.990e+0
	A2	-4.211e-2	4.220e-3	-1.259e-2	1.911e+0
	A3	1.633e-2	2.935e-2	-4.108e-2	1.700e+0
152	A1	1.333e-1	1.164e-2	-7.204e-3	1.860e+0
	A2	-3.931e-2	4.356e-3	-1.367e-2	2.083e+0
	A3	1.905e-2	3.707e-2	-5.834e-1	1.626e+0
153	A1	1.336e-1	1.102e-2	-4.250e-2	1.851e+0
	A2	-3.932e-2	4.349e-3	-1.657e-2	2.031e+0
	A3	1.806e-2	3.419e-2	1.973e+0	1.636e+0
154	A1	1.332e-1	1.024e-2	2.231e-2	2.392e+0
	A2	-3.931e-2	4.379e-3	-1.384e-2	2.075e+0
	A3	1.909e-2	3.018e-2	-7.891e-1	1.815e+0
155	A1	1.331e-1	1.020e-2	1.734e-2	1.877e+0
	A2	-4.190e-2	4.966e-3	-1.776e-2	1.833e+0
	A3	1.619e-2	3.444e-2	7.861e-1	1.720e+0
156	A1	1.332e-1	1.151e-2	4.449e-2	1.969e+0
	A2	-4.198e-2	3.579e-3	1.197e-3	2.317e+0
	A3	1.632e-2	3.385e-2	-7.228e-1	1.733e+0
157	A1	1.336e-1	1.227e-2	-8.458e-2	2.116e+0
	A2	-4.212e-2	3.694e-3	2.737e-4	2.262e+0
	A3	1.552e-2	3.833e-2	1.665e+0	1.881e+0
158	A1	1.333e-1	1.108e-2	2.076e-2	2.079e+0
	A2	-4.220e-2	3.609e-3	-3.715e-4	2.219e+0
	A3	1.636e-2	3.364e-2	-1.389e+0	1.700e+0
159	A1	1.333e-1	1.043e-2	5.799e-2	2.257e+0
	A2	-4.222e-2	3.664e-3	-3.211e-3	2.180e+0
	A3	1.659e-2	3.162e-2	-3.887e-1	1.598e+0
160	A1	1.335e-1	9.800e-3	2.929e-2	2.180e+0
	A2	-4.261e-2	2.918e-3	-4.836e-3	2.600e+0

Table 12: *Mean, standard deviation, skewness and kurtosis of the measurements in each directions.*

FRACTURE AND DYNAMICS PAPERS

PAPER NO. 33: A. Rytter, R. Brincker & L. Pilegaard Hansen: *Detection of Fatigue Damage in a Steel Member.* ISSN 0902-7513 R9138.

PAPER NO. 34: J. P. Ulfkjær, S. Krenk & R. Brincker: *Analytical Model for Fictitious Crack Propagation in Concrete Beams.* ISSN 0902-7513 R9206.

PAPER NO. 35: J. Lyngbye: *Applications of Digital Image Analysis in Experimental Mechanics.* Ph.D.-Thesis. ISSN 0902-7513 R9227.

PAPER NO. 36: J. P. Ulfkjær & R. Brincker: *Indirect Determination of the $\sigma - w$ Relation of HSC Through Three-Point Bending.* ISSN 0902-7513 R9229.

PAPER NO. 37: A. Rytter, R. Brincker & P. H. Kirkegaard: *An Experimental Study of the Modal Parameters of a Damaged Cantilever.* ISSN 0902-7513 R9230.

PAPER NO. 38: P. H. Kirkegaard: *Cost Optimal System Identification Experiment Design.* ISSN 0902-7513 R9237.

PAPER NO. 39: P. H. Kirkegaard: *Optimal Selection of the Sampling Interval for Estimation of Modal Parameters by an ARMA-Model.* ISSN 0902-7513 R9238.

PAPER NO. 40: P. H. Kirkegaard & R. Brincker: *On the Optimal Location of Sensors for Parametric Identification of Linear Structural Systems.* ISSN 0902-7513 R9239.

PAPER NO. 41: P. H. Kirkegaard & A. Rytter: *Use of a Neural Network for Damage Detection and Location in a Steel Member.* ISSN 0902-7513 R9245

PAPER NO. 42: L. Gansted: *Analysis and Description of High-Cycle Stochastic Fatigue in Steel.* Ph.D.-Thesis. ISSN 0902-7513 R9135.

PAPER NO. 43: M. Krawczuk: *A New Finite Element for Static and Dynamic Analysis of Cracked Composite Beams.* ISSN 0902-7513 R9305.

PAPER NO. 44: A. Rytter: *Vibrational Based Inspection of Civil Engineering Structures.* Ph.D.-Thesis. ISSN 0902-7513 R9314.

PAPER NO. 45: P. H. Kirkegaard & A. Rytter: *An Experimental Study of the Modal Parameters of a Damaged Steel Mast.* ISSN 0902-7513 R9320.

PAPER NO. 46: P. H. Kirkegaard & A. Rytter: *An Experimental Study of a Steel Lattice Mast under Natural Excitation.* ISSN 0902-7513 R9326.

PAPER NO. 47: P. H. Kirkegaard & A. Rytter: *Use of Neural Networks for Damage Assessment in a Steel Mast.* ISSN 0902-7513 R9340.

PAPER NO. 48: R. Brincker, M. Demosthenous & G. C. Manos: *Estimation of the Coefficient of Restitution of Rocking Systems by the Random Decrement Technique.* ISSN 0902-7513 R9341.

PAPER NO. 49: L. Gansted: *Fatigue of Steel: Constant-Amplitude Load on CCT-Specimens.* ISSN 0902-7513 R9344.

FRACTURE AND DYNAMICS PAPERS

PAPER NO. 50: P. H. Kirkegaard & A. Rytter: *Vibration Based Damage Assessment of a Cantilever using a Neural Network.* ISSN 0902-7513 R9345.

PAPER NO. 51: J. P. Ulfkjær, O. Hededal, I. B. Kroon & R. Brincker: *Simple Application of Fictitious Crack Model in Reinforced Concrete Beams.* ISSN 0902-7513 R9349.

PAPER NO. 52: J. P. Ulfkjær, O. Hededal, I. B. Kroon & R. Brincker: *Simple Application of Fictitious Crack Model in Reinforced Concrete Beams. Analysis and Experiments.* ISSN 0902-7513 R9350.

PAPER NO. 53: P. H. Kirkegaard & A. Rytter: *Vibration Based Damage Assessment of Civil Engineering Structures using Neural Networks.* ISSN 0902-7513 R9408.

PAPER NO. 54: L. Gansted, R. Brincker & L. Pilegaard Hansen: *The Fracture Mechanical Markov Chain Fatigue Model Compared with Empirical Data.* ISSN 0902-7513 R9431.

PAPER NO. 55: P. H. Kirkegaard, S. R. K. Nielsen & H. I. Hansen: *Identification of Non-Linear Structures using Recurrent Neural Networks.* ISSN 0902-7513 R9432.

PAPER NO. 56: R. Brincker, P. H. Kirkegaard, P. Andersen & M. E. Martinez: *Damage Detection in an Offshore Structure.* ISSN 0902-7513 R9434.

PAPER NO. 57: P. H. Kirkegaard, S. R. K. Nielsen & H. I. Hansen: *Structural Identification by Extended Kalman Filtering and a Recurrent Neural Network.* ISSN 0902-7513 R9433.

PAPER NO. 58: P. Andersen, R. Brincker, P. H. Kirkegaard: *On the Uncertainty of Identification of Civil Engineering Structures using ARMA Models.* ISSN 0902-7513 R9437.

PAPER NO. 59: P. H. Kirkegaard & A. Rytter: *A Comparative Study of Three Vibration Based Damage Assessment Techniques.* ISSN 0902-7513 R9435.

PAPER NO. 60: P. H. Kirkegaard, J. C. Asmussen, P. Andersen & R. Brincker: *An Experimental Study of an Offshore Platform.* ISSN 0902-7513 R9441.

PAPER NO. 61: R. Brincker, P. Andersen, P. H. Kirkegaard, J. P. Ulfkjær: *Damage Detection in Laboratory Concrete Beams.* ISSN 0902-7513 R9458.

PAPER NO. 62: R. Brincker, J. Simonsen, W. Hansen: *Some Aspects of Formation of Cracks in FRC with Main Reinforcement.* ISSN 0902-7513 R9506.

PAPER NO. 63: R. Brincker, J. P. Ulfkjær, P. Adamsen, L. Langvad, R. Toft: *Analytical Model for Hook Anchor Pull-out.* ISSN 0902-7513 R9511.

Department of Building Technology and Structural Engineering
Aalborg University, Sohngaardsholmsvej 57, DK 9000 Aalborg
Telephone: +45 98 15 85 22 Telefax: +45 98 14 82 43